

Calculations for finding limit conditions in shipboard machinery installation

Auteur : Florido Sánchez, Adrián

Promoteur(s) : Rigo, Philippe

Faculté : Faculté des Sciences appliquées

Diplôme : Master : ingénieur civil mécanicien, à finalité spécialisée en "Advanced Ship Design"

Année académique : 2023-2024

URI/URL : <http://hdl.handle.net/2268.2/22243>

Avertissement à l'attention des usagers :

Tous les documents placés en accès ouvert sur le site le site MatheO sont protégés par le droit d'auteur. Conformément aux principes énoncés par la "Budapest Open Access Initiative"(BOAI, 2002), l'utilisateur du site peut lire, télécharger, copier, transmettre, imprimer, chercher ou faire un lien vers le texte intégral de ces documents, les disséquer pour les indexer, s'en servir de données pour un logiciel, ou s'en servir à toute autre fin légale (ou prévue par la réglementation relative au droit d'auteur). Toute utilisation du document à des fins commerciales est strictement interdite.

Par ailleurs, l'utilisateur s'engage à respecter les droits moraux de l'auteur, principalement le droit à l'intégrité de l'oeuvre et le droit de paternité et ce dans toute utilisation que l'utilisateur entreprend. Ainsi, à titre d'exemple, lorsqu'il reproduira un document par extrait ou dans son intégralité, l'utilisateur citera de manière complète les sources telles que mentionnées ci-dessus. Toute utilisation non explicitement autorisée ci-avant (telle que par exemple, la modification du document ou son résumé) nécessite l'autorisation préalable et expresse des auteurs ou de leurs ayants droit.

Universität
Rostock



Traditio et Innovatio



With the support of the
Erasmus+ Programme
of the European Union

Calculations for finding limit conditions in shipboard machinery installation

submitted on 05 August 2024

by

FLORIDO SANCHEZ Adrián | Caprivistraße 18A | 24105 Kiel | adrian.sanchez@uni-rostock.de

Student ID No.: 223 202 136

First Reviewer:

Prof. Dr. Eng./ Hiroshima Univ. Patrick Kaeding
University of Rostock
Faculty of Mechanical Engineering
and Marine Technology
Chair of Ship Structures
Albert-Einstein-Str. 2
18059 Rostock

Second Reviewer:

Dr. Dietrich Wittekind
DW ShipConsult GmbH
Lise-Meitner-Str. 9
24223 Schwentinental



Master Thesis

CONTENTS

1. INTRODUCTION..... 7

1.1 Motivation 7

1.2 Objectives..... 7

2. METHODOLOGY 9

2.1 Ship Noise Theory..... 9

2.2 SNAME’s Empirical Method..... 11

2.2.1 *Structure-borne Noise Transmission*..... 11

2.2.2 *Limitations*..... 14

2.3 Finite Element Method..... 15

2.3.1 *Harmonic Analysis* 15

2.3.2 *Geometry* 18

2.3.3 *Meshing* 19

2.3.4 *Loading Cases* 25

2.3.5 *Calculation Points*..... 26

3. RESULTS..... 28

3.1 Transmission Losses Calculation 28

3.1.1 *From Foundation to Effective Source Area* 28

3.1.2 *From Effective Source Area to Deck (Top)*..... 31

3.1.3 *From Effective Source Area to Deck (Side)* 33

3.1.4 *Comparison SNAME and FEM* 34

3.2 Limit Conditions in Shipboard Machinery Installation..... 36

3.3 Comparison Between Foundations..... 44

4. CONCLUSIONS 48

5. REFERENCES 49

LIST OF FIGURES

Figure 1. AIDAprima in the port of Kiel.	8
Figure 2. A-weighting filtering curve.	11
Figure 3. Source room layout.	12
Figure 4. Structure-borne sound transmission path.	14
Figure 5. Mass-spring-damper single degree of freedom system.	15
Figure 6. Geometry of the engine room.	18
Figure 7. Bending wavelength of steel plates.	19
Figure 8. Thicknesses of the shell elements.	20
Figure 9. Modal analysis simply supported beam.	21
Figure 10. Modal analysis convergence plot.	21
Figure 11. Mesh at the engine foundation.	23
Figure 12. Mesh metrics.	24
Figure 13. Loading cases 1 and 2.	25
Figure 14. Loading cases 3 and 4.	25
Figure 15. Location of the foundation and the effective source area.	26
Figure 16. Location of the deck (top) and deck (side).	26
Figure 17. Location of the calculation points on the foundation.	27
Figure 18. Frequency response function: foundation and effective source area.	28
Figure 19. Transmission losses from foundation to effective source area.	29
Figure 20. Response of the structure at 74 Hz and 158,6 Hz.	29
Figure 21. Response at the location of the foundation at 74 Hz and 158,6 Hz.	30
Figure 22. Response of the structure at 232,2 Hz and 452,6 Hz.	30
Figure 23. Response at the location of the foundation at 232,2 Hz and 452,6 Hz.	31
Figure 24. Frequency response function: effective source area and deck (top).	31
Figure 25. Transmission losses from effective source area to deck (top).	32
Figure 26. Response of the structure at 14,6 Hz and 19,5 Hz.	32
Figure 27. Frequency response function: effective source area and deck (side).	33
Figure 28. Transmission losses from effective source area to deck (side).	33
Figure 29. Response of the structure at 21,4 Hz and 45,9 Hz.	34
Figure 30. Airborne noise on deck (top) according to SNAME and FEM.	35
Figure 31. Engine foundation initial geometry.	36
Figure 32. Calculation points for the first load case.	37
Figure 33. Transfer function between point 1 and 2.	37

Figure 34. Transfer function between point 1 and 3.	38
Figure 35. Transfer function between point 1 and 4.	38
Figure 36. Calculation points for the second load case.	39
Figure 37. Transfer function between point 2 and 3.	39
Figure 38. Transfer function between point 2 and 4.	40
Figure 39. Calculation points for the third load case.	40
Figure 40. Transfer function between point 3 and 4.	41
Figure 41. Average of the six transfer functions for both foundations.	41
Figure 42. Frequency response foundation at the engine foundation.	44
Figure 43. Frequency response foundation at the effective source area.	45
Figure 44. Frequency response foundation at deck (top).	45
Figure 45. Frequency response foundation at deck (side).	46
Figure 46. Airborne noise on deck (top) for both foundations.	46
Figure 47. Frequency response function: weak foundation and effective source area.	47

LIST OF TABLES

Table 1. Transmission loss from foundation top to deck plate	12
Table 2. Influence of the number of elements per half wavelength on accuracy.....	22
Table 3. Vibration velocity levels on the foundation top	34
Table 4. Reduction of scantling in the engine foundation.....	36
Table 5. Noise amplification	42
Table 6. Vibration velocity levels on the foundation top for the weak foundation.....	42
Table 7. Noise Level Limits, dB(A).....	42

DECLARATION OF AUTHORSHIP

I declare that this thesis and the work presented in it are my own and have been generated by me as the result of my own original research.

Where I have consulted the published work of others, this is always clearly attributed.

Where I have quoted from the work of others, the source is always given. With the exception of such quotations, this thesis is entirely my own work.

I have acknowledged all main sources of help.

Where the thesis is based on work done by myself jointly with others, I have made clear exactly what was done by others and what I have contributed myself.

This thesis contains no material that has been submitted previously, in whole or in part, for the award of any other academic degree or diploma.

I cede copyright of the thesis in favour of the University of Rostock.

Date: 05/08/2024

Signature



ABSTRACT

This master thesis presents the noise assessment of the structure of the engine room of a cruise ship. The structure under analysis is made up of two decks, double bottom, double side and one bulkhead and different pillars connecting both decks. The study is performed using an empirical method and the finite element method. This investigation is carried out because of the necessity to find limit conditions in shipboard machinery installation during the design phase since fixing noise-related issues after construction is expensive and difficult to address.

The empirical method provides a fast check of the noise assessment. However, this method presents some limitations which could provide wrong results if the method is applied out of range. The results from the finite element analysis allow to identify these limitations and correct the results. The detailed elaboration of the finite element model (type of model, geometry, meshing, loading cases) is a fundamental aspect of this thesis.

In general, engine suppliers give as an input the noise generated by the engine on top of the test engine foundation. But designers are not interested in this value since the engine foundation on the ship has not the same characteristics and hence the noise will be different which could cause a violation of limit conditions in shipboard machinery installation. A methodology is developed to estimate the how changes in the foundation influence the noise.

Finally, the engine foundation is modified to understand how changes in this part of the structure influence the noise propagation in the entire structure. The results from both foundations is compared.

1. INTRODUCTION

1.1 Motivation

Noise on board ships and offshore units has seen increased attention in recent years. Excessive noise levels can adversely affect crew members' health and their task performance. Crew members may become distracted if exposed to high noise and vibration levels and this can increase the potential for human error. Prolonged exposure to high-noise environments can lead to long-term health issues such as noise induced hearing loss. It is expensive and difficult to fix noise-related issues after construction. Therefore, it is important and necessary for designers and builders to perform noise analyses and address these concerns at an early design stage.

For onboard noise analysis of ship and offshore units, the commonly adopted "Source-Path-Receiver" modelling technique may be used. This modelling scheme takes three key elements into consideration: noise sources, transmission paths, and the receiver acoustic characteristics. "Sources" are the equipment which generates airborne noise and structure-borne noise, such as main engines, propellers, compressors, and fans. "Paths" are the air, fluid, or solid structures such as deck and bulkheads through which sound propagates. "Receivers" are the compartment of interest, such as crew cabins, workspaces, and offices.

Empirical methods and numerical analysis methods can be used to calculate the sound attenuation from "Sources" to "Receivers" through different transmission "Paths". Various empirical methods have been developed. For example, The Society of Naval Architects and Marine Engineers (SNAME) published the *Design Guide for Shipboard Airborne Noise Control* (SNAME, 2019), which provides a step-by-step empirical method to predict onboard ship noise levels. (ABS, 2019)

1.2 Objectives

Some types of ships such as cruise ships (Fig. 1) feature a very demanding requirement on board noise. The main task of this thesis is to study how the structure-borne noise is propagated through the ship structure to find limit conditions in shipboard machinery installation. In order to perform the analysis, the engine room structure of a cruise ship will be studied. The main objectives of this thesis are established here below:

- Firstly, the structure-borne noise propagation will be studied using both the SNAME's empirical method and the Finite Element Method (FEM). The obtained results will be

compared in order to show the limitations of the method proposed by SNAME. The analysis will cover the first five frequency bands (31,5 Hz, 63 Hz, 125 Hz, 250 Hz, 500 Hz).

- Secondly, the geometry of the engine foundation will be modified. The idea is to study how changes in this element influence the structure-borne noise propagation. A methodology to predict the variation of the noise levels will be developed in order to find limit conditions in shipboard machinery installation.
- Finally, the results obtained from the two different geometries will be compared to show how the structure-borne noise propagation is modified.



Figure 1. AIDAprima in the port of Kiel. Available from <https://www.portofkiel.com/news-reader-en/kiel-week-kick-off-with-aidaluna.html> [Accessed 15 July 2024].

2. METHODOLOGY

2.1 Ship Noise Theory

In acoustics, the level of a quantity is the logarithm of the ratio of that quantity to a reference quantity of the same kind. The base of the logarithm, the reference quantity, and the kind of level need to be specified. Examples are sound power levels, sound pressure levels, acceleration levels, and velocity levels. Levels are always expressed in decibels (dB). Structure-borne noise can be expressed in terms of vibration velocity level L_v which is defined as:

$$L_v = 20 \cdot \log \frac{v}{v_0} \quad (1)$$

Where:

- v = vibration velocity generated by the excitation source, in m/s
- v_0 = standard reference velocity, 5×10^{-8} m/s.

The total path transfer function or transmission loss along any particular structural path (A-B) is determined as follows:

$$TF_{path} = 20 \cdot \log v_A - 20 \cdot \log v_B \quad (2)$$

The frequency range of onboard noise analyses for ships and offshore units is usually from 31,5 Hz to 8000 Hz. Considering the large span of the frequency range, it is usually subdivided into frequency bands. The most common one is the octave frequency band (ABS, 2019). The centre frequencies of the octave bands for onboard noise analyses are typically: 31,5 Hz, 63 Hz, 125 Hz, 250 Hz, 500 Hz, 1000 Hz, 2000 Hz, 4000 Hz and 8000 Hz. The following equations show the relationship between centre frequency and upper/lower frequency of an octave band:

$$\frac{f_u}{f_l} = 2 \quad (3)$$

$$f_c = \sqrt{f_u \cdot f_l} \quad (4)$$

Where:

- f_u = upper bound frequency, in Hz
- f_l = lower bound frequency, in Hz

f_c = centre frequency, in Hz.

The radiation efficiency of the structure relates the vibration level on the plates to the radiated airborne noise. The sound pressure levels L_p radiated by a vibrating structure depends on the amplitude of the vibration, the size of the vibrating structure, and the details of surface motion. Radiated power is calculated as follows:

$$p^2 = v^2 \cdot \rho^2 \cdot c^2 \cdot \sigma \quad (5)$$

$$L_p = 20 \cdot \log \frac{p}{p_0} = 10 \cdot \log \left(\frac{v^2}{v_0^2} \right) + 10 \cdot \log(\rho^2) + 10 \cdot \log(c^2) + 10 \cdot \log(\sigma) \quad (6)$$

Where:

p = sound pressure measured at a certain location, in Pa
 p_0 = standard reference pressure, 2×10^{-5} Pa
 ρ = density of air, 1,22 kg/m³
 c = the sound speed in air, 340 m/s
 σ = radiation efficiency of a plate.

$$\sigma = \frac{U \cdot c}{\pi^2 \cdot S \cdot f_c} \cdot \sqrt{\frac{f}{f_c}} \quad f < f_c \quad (7)$$

$$\sigma = 1 \quad f > f_c \quad (8)$$

Where:

U = circumference of stiffeners around area, in m
 S = area between stiffeners, in m²
 f_c = coincidence frequency, in Hz.

$$f_c = \frac{c^2}{1,8 \cdot c_l \cdot h} \quad (9)$$

Where:

c_l = longitudinal sound velocity in steel, 5000 m/s
 h = plate thickness, in m.

The human ear is not equally sensitive to all frequencies of sound. To the human ear, a low frequency sound is quieter than a high frequency sound of the same level. Therefore, in onboard noise analysis for ships and offshore units, A-weighting is used to take this into consideration. It approximates the sensitivity of the human ear by filtering these frequencies. A-weighted decibels are abbreviated dB(A). (ABS, 2019)

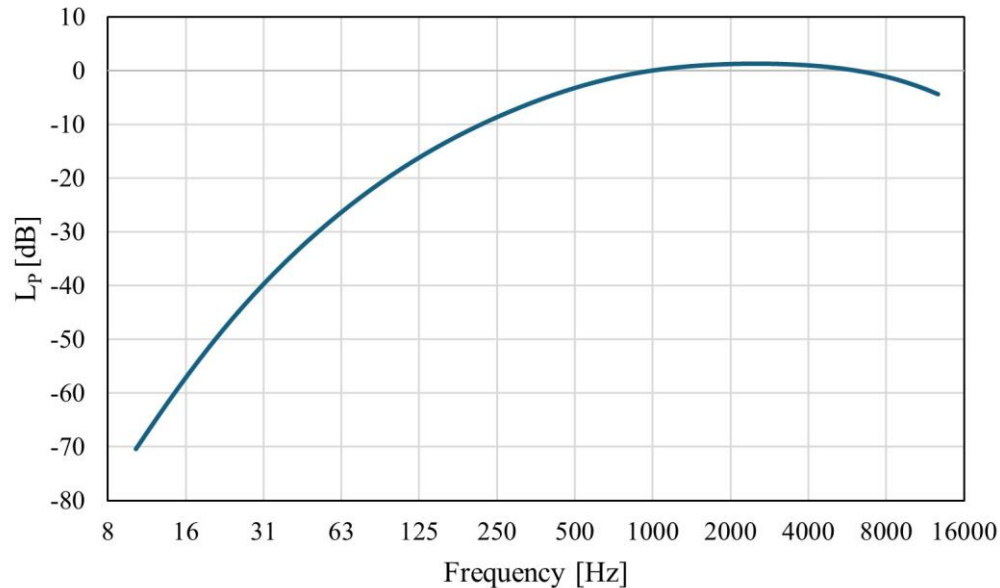


Figure 2. A-weighting filtering curve.

In general, engine suppliers specify the structure-borne noise at the top of the engine foundation. So, this value is considered as the input in the analysis. Then, it is necessary to determine the transmission losses between the source and the receiver compartment. Finally, the radiation efficiency and A-weighting is applied to obtain the A-weighted sound pressure levels which are used for the comparison with the criteria.

2.2 SNAME's Empirical Method

2.2.1 Structure-borne Noise Transmission

Practical information on the acoustical design of ships is provided in a simple, usable format that requires little prior experience with acoustical experience. The mathematics employed in the prediction procedures in this document is limited to elementary algebra and the manipulation of logarithmically based sound and vibration levels. The elements of the structure-borne path in ships can be divided into four groups, as listed below:

- Structures within the source room.

- Structures beyond the source room.
- Intersection of structures
- Pillars.

Within the source room (Fig. 3), the structure-borne transmission loss from an effective source area to the source room boundary mainly depends on its shape, orientation, and distance to the compartment boundary. “Effective source area” is the deck region immediately below the machinery’s foundation. The transmission losses (TL) from the foundation top plate to deck plate around the foundation are tabulated in Table 1. Negative values mean amplification.

Table 1. Transmission loss from foundation top to deck plate.

Freq. (Hz)	31,5	63	125	250	500	1000	2000	4000	8000
TL (dB)	-10	-13	-13	-10	-7	-5	-2	0	0

Once the noise level is determined in the deck region below the foundation, the transmission loss within the source room ΔL_a can be calculated by the formula below:

$$\Delta L_a = 10 \cdot \log \left(\frac{(r_1 + r_2) \cdot (1 - 0,35 \cdot \varepsilon_r)}{(a + 2 \cdot r_{fr}) \cdot (1 - 0,35 \cdot \varepsilon_0)} \right) \quad (10)$$

$$\varepsilon_0 = \frac{(a - b) \cdot (a + b + 4 \cdot r_{fr})}{(a + 2 \cdot r_{fr})^2} \quad (11)$$

$$\varepsilon_r = \frac{(a - b) \cdot (a + b + 4 \cdot r_{fr})}{(r_1 + r_2)^2} \quad (12)$$

Where:

- r_i = distance from the ends of the effective source area, in m
- a = length of the effective source area, in m
- b = width of the effective source area, in m
- r_{fr} = minimum frame spacing, in m.

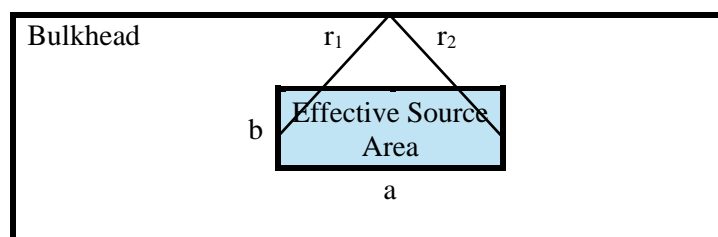


Figure 3. Source room layout.

For the structure beyond the source room, the structure-borne transmission loss depends on the damping loss factor of the structure, the size of the structure, and the distance from source to the structure of interest. The transmission loss beyond the source room ΔL_d can be calculated by the formula below:

$$\Delta L_d = 0,066 \cdot \sqrt{f} \cdot \sum_N \frac{l_i \cdot \eta_i}{\sqrt{t_i}} \quad (13)$$

Where:

- f = octave band frequency of interest, in Hz
- N = “structures” between the source room and the structure of interest
- l_i = size of the i^{th} structure, in m
- η_i = damping loss factor of the i^{th} structure
- t_i = thickness of the i^{th} structural element plating, in m
- i = number of the structure.

For the intersection of structures, such as the junction of two bulkheads, bulkhead and deck, or a deck and the hull, the structure-borne transmission loss can be significant. The transmission loss of the intersection depends primarily on three factors: the shape of the intersection, the plate thickness, and the material. The higher number of intersections between the source and the receiver along the transmission path, the more the structure-borne sound attenuates. The transmission loss caused by all intersections TL_{inter} can be calculated by the formula below:

$$TL_{inter} = \sum_N \frac{TL_n}{\sqrt{n}} \quad (14)$$

$$TL_n = 10 \cdot \log \frac{1}{\tau_{ij}} \quad (15)$$

$$\tau_{ij} = \frac{2 \cdot \left(\frac{t_j}{t_i}\right)^{1,5}}{\left(1 + \sum_{k=2}^{k=M} \frac{\rho_k \cdot t_k^{2,5}}{\rho_i \cdot t_i^{2,5}}\right)^2} \quad (16)$$

Where:

- N = number of connections between the source and receiver
- n = connection number
- TL_n = transmission loss for the n^{th} intersection, in dB

- ρ = is the density of the metal plate
 t = is the thickness of the metal plate
 i = subscript i is for the plate with the oncoming energy
 j = subscript j is the plate receiving the energy
 M = type of connection (SNAME, 2019).

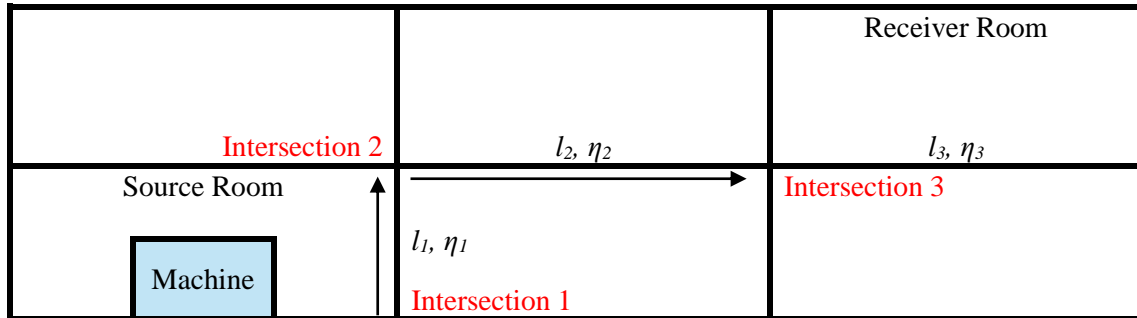


Figure 4. Structure-borne sound transmission path.

Pillars usually act as a rigid coupling between decks at most frequencies of interest. Therefore, pillars, especially those located in the vicinity of vibration sources, cannot be ignored in the noise analysis as the acoustic energy can transmit through the pillar with almost no dissipation.

The total path transfer function for any single piece of equipment along any particular structural path TF_{path} is determined as:

$$TF_{path} = \Delta L_a + \Delta L_d + TL_{inter} \quad (17)$$

2.2.2 Limitations

The data and analytical techniques presented in this procedure have some limitations. Some simplifications and approximations are necessary to make the procedures amenable to simple calculations. Also, in the frequency range below the 125 Hz octave band, reliable data for source characteristics and path attenuation effects are very difficult to obtain. Thus, much of the data and many of the scaling laws for the range below 125 Hz have been extrapolated from higher frequency information.

Because a larger noise data base exists for Navy equipment than for commercial equipment because of the Navy's noise reduction programs, the user must be aware that much of the information used in this guide to predict machinery noise levels is based on standard U.S.

Navy equipment, which is much quieter and generally much more expensive than commercial marine equipment.

This document cannot assist the user in analysing every situation that may arise, specifically in the case of structure-borne noise. The procedures used in the guide are based on generalized models of ship structures and cannot possibly include all of the complex configurations that could occur in all kinds of ship structures.

2.3 Finite Element Method

2.3.1 Harmonic Analysis

As it was established in the theoretical background (Section 2.1), the starting point of the analysis are the vibration velocity levels. Vibration is a complex phenomenon happening on ship and machinery space. To understand and have the first sight of vibration assessment, the fundamental vibration theory is introduced. A single degree of freedom (SDOF) system, consisting of mass-spring-damper, is often used to understand dynamic systems and their properties as shown here below. (SIEMENS, 2019)

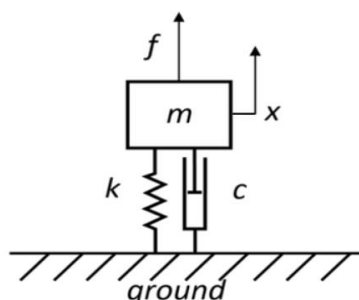


Figure 5. Mass-spring-damper single degree of freedom system. Available from https://support.sw.siemens.com/en-US/okba/KB000036272_EN_US/Natural-Frequency-and-Resonance/index.html

[Accessed 16 July 2024].

SDOF vibration can be analysed by Newton's second law of motion. The analysis can be easily visualized with the aid of a free body diagram. The resulting equation of motion is a 2nd order linear differential equation which describes the forced response.

$$m \cdot \ddot{x} + c \cdot \dot{x} + k \cdot x = f(t) \quad (18)$$

Where:

- m = mass of the system, in kg
- c = damping of the system, in Ns/m

k	=	stiffnes, in N/m
x	=	displacement, in m
f	=	force applied to system, in N.

The undamped natural vibration case ($c=0, f=0$) allows to calculate the natural frequency w_n of the system. High amplitude vibrations will follow if the frequency of the excitation force w match the natural frequency.

$$w_n = \sqrt{\frac{k}{m}} \quad (19)$$

The huge number of degrees of freedom that are required in the shipbuilding industry makes the analysis more complex but the concepts from the SDOF are still valid. The finite element method allows the study of the forced response from simple beams to ship models. Harmonic analysis is used to determine the response of the structure under a steady-state sinusoidal (harmonic) loading at a given frequency. The idea is to calculate the structure's response at several frequencies and obtain a graph of some response quantity versus frequency which is known as frequency response function. Harmonic response analysis allows to predict the dynamic behaviour of the structure, thus enabling to verify whether or not the design will successfully overcome the harmful effects of forced vibrations. The general equation of motion solved by the FEM is provided:

$$[M]\{\ddot{x}\} + [C]\{\dot{x}\} + [K]\{x\} = \{F(t)\} \quad (20)$$

Where:

$[M]$	=	structural mass matrix
$[C]$	=	structural damping matrix
$[K]$	=	structural damping matrix
$\{\ddot{x}\}$	=	nodal acceleration vector
$\{\dot{x}\}$	=	nodal velocity vector
$\{x\}$	=	nodal displacement vector
$\{F(t)\}$	=	applied load vector.

Complex numbers are introduced to simplify the analysis. Starting from a force which is certain constant times cosine function. Such force can be written as the real part of a complex number:

$$F = F_0 \cdot \cos(w \cdot t) \quad (21)$$

$$\hat{F} = F_0 \cdot e^{i\omega t} \quad (22)$$

$$e^{i\omega t} = \cos(w \cdot t) + i \cdot \sin(w \cdot t) \quad (23)$$

The reason to do this is that it is easier to work with an exponential function than with a cosine. So, the whole trick is to represent the oscillatory function as the real part of a complex number. The complex number \hat{F} is not a real physical force, because no force in physics is really complex. However, \hat{F} is denoted as a force, but of course the actual force is the real part of that expression. If now the force presents a phase shift ψ , the force can be written as:

$$F = F_0 \cdot \cos(w \cdot t + \psi) \quad (24)$$

$$\hat{F} = F_0 \cdot e^{i(\omega t + \psi)} = F_0 \cdot e^{i\omega t} \cdot e^{i\psi} \quad (25)$$

$$\hat{F} = [F_0 \cdot (\cos(\psi) + i \cdot \sin(\psi))] \cdot e^{i\omega t} \quad (26)$$

$$\hat{F} = [F_1 + i \cdot F_2] \cdot e^{i\omega t} \quad (27)$$

Thus, it is clear that the algebra of exponentials is much easier than that of sines and cosines. This is the reason to use complex numbers for the analysis. Therefore, the displacement and force vectors can be rewritten as:

$$\{x\} = (\{u_1\} + i \cdot \{u_2\}) \cdot e^{i\omega t} \quad (28)$$

$$\{F(t)\} = (\{F_1\} + i \cdot \{F_2\}) \cdot e^{i\omega t} \quad (29)$$

Substituting these expressions into the equation of motion gives:

$$([K] - w^2 \cdot [M] + iw \cdot [C]) \cdot (\{u_1\} + i \cdot \{u_2\}) \cdot e^{i\omega t} = (\{F_1\} + i \cdot \{F_2\}) \cdot e^{i\omega t} \quad (30)$$

The dependence on time is the same on both sides of the equation and may therefore be removed:

$$([K] - w^2 \cdot [M] + iw \cdot [C]) \cdot (\{u_1\} + i \cdot \{u_2\}) = (\{F_1\} + i \cdot \{F_2\}) \quad (31)$$

The full solution method solves the last equation directly. It may be expressed as:

$$[K_c] \cdot \{u_c\} = \{F_c\} \quad (32)$$

Where c denotes a complex matrix or vector. This equation is solved using the same procedures that are used for a static analysis, except that for the harmonic analysis the use of complex arithmetic is done. (ANSYS1, 2017)

2.3.2 Geometry

The geometry of the engine room (Fig. 6) consists of a double bottom, double side and two decks connected by one bulkhead and different pillars. Additionally, the symmetry conditions of the geometry are taken into consideration. The structural model represents the primary supporting members with the plating to which they are connected. Ordinary stiffeners are also represented in the model to reproduce the stiffness and inertia of the structure.

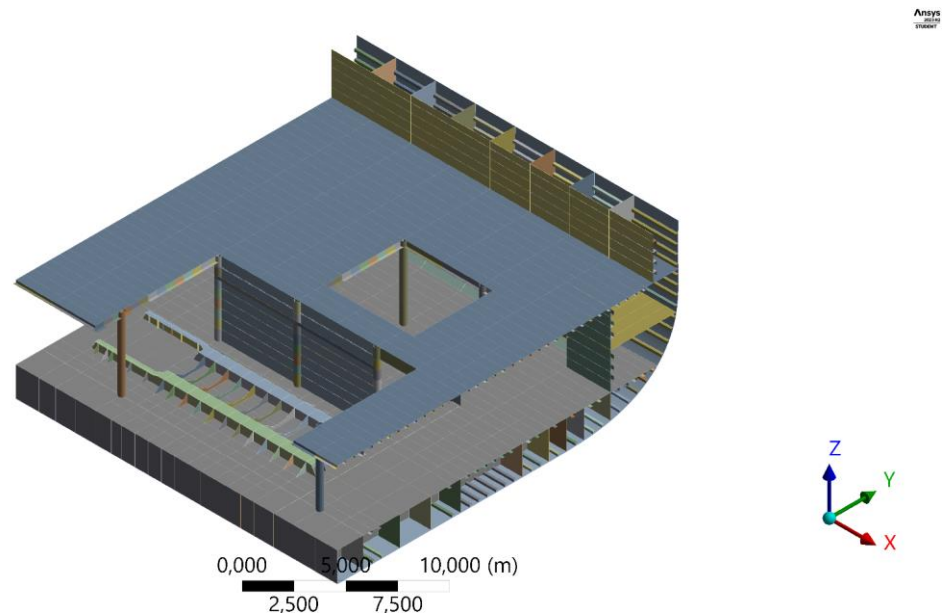


Figure 6. Geometry of the engine room.

A plate is a thin solid and might be modelled by 3D solid elements. However, a solid element is wasteful of degrees of freedom as it computes transverse normal stress and transverse shear stresses, all of which are considered negligible in a thin plate. For this reason, shell elements are used to model thin structures (where one dimension is much smaller than the other two dimensions). Shell elements are usually created by meshing a surface representing the position and shape of the structure and associating them with section data to represent shell thickness and properties. Only plane stress is allowed in shell elements. In this structural model the primary supporting members and plates are modelled as shell elements. (ANSYS2, 2017)

Ordinary stiffeners are represented by beam elements which are line elements used to create 1D idealization of a 3D structure. They are computationally more efficient than solids and shells. (ANSYS3, 2017)

2.3.3 Meshing

Structure borne sound relates to the sound waves pulsating and radiating through a solid structure. For this analysis the sound waves in steel plates are of special interest due to the ship structure is mainly composed of plates. Therefore, the main target is to represent the bending wavelength of the plates accurately. Figure 7 shows the bending wavelength as a function of frequency.

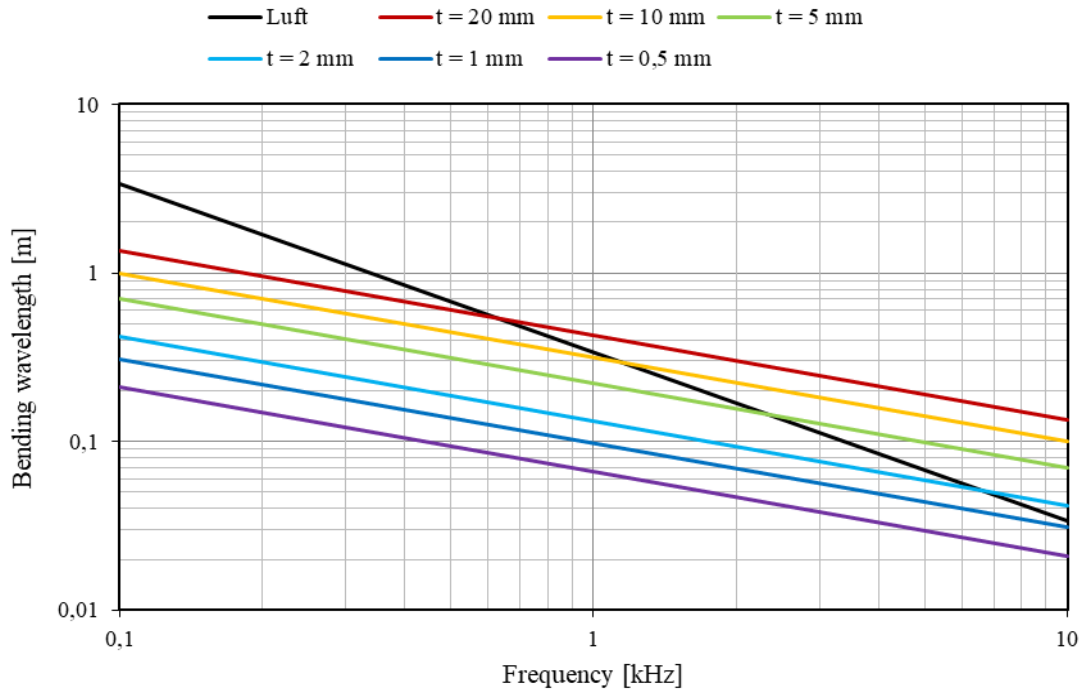


Figure 7. Bending wavelength of steel plates.

Clearly, the wavelength decreases as frequency increases. On the other hand, the wavelength increases for thick plates. As a result, the smallest wavelength will be obtained for the element with smallest thickness at the highest frequency of study. The following expression gives the bending wavelength for a given thickness and frequency.

$$\lambda = \sqrt[4]{\frac{4 \cdot \pi^2 \cdot B}{f^2 \cdot m}} = \sqrt[4]{\frac{4 \cdot \pi^2 \cdot \frac{E \cdot h^3}{12 \cdot (1 - \mu^2)}}{f^2 \cdot h \cdot \rho}} \quad (33)$$

Where:

- B = bending stiffness of a plate
- f = frequency of interest, in Hz
- m = mass per unit of area, in kg/m²

E	=	Young's modulus, in Pa
h	=	plate thickness, in m
μ	=	Poisson's ratio
ρ	=	material density, in kg/m ³ .

In order to perform the analysis until the frequency band of 500 Hz and knowing that the smaller plates thickness is 8 mm (Fig. 8), the resulting bending wavelength is of 330 mm.

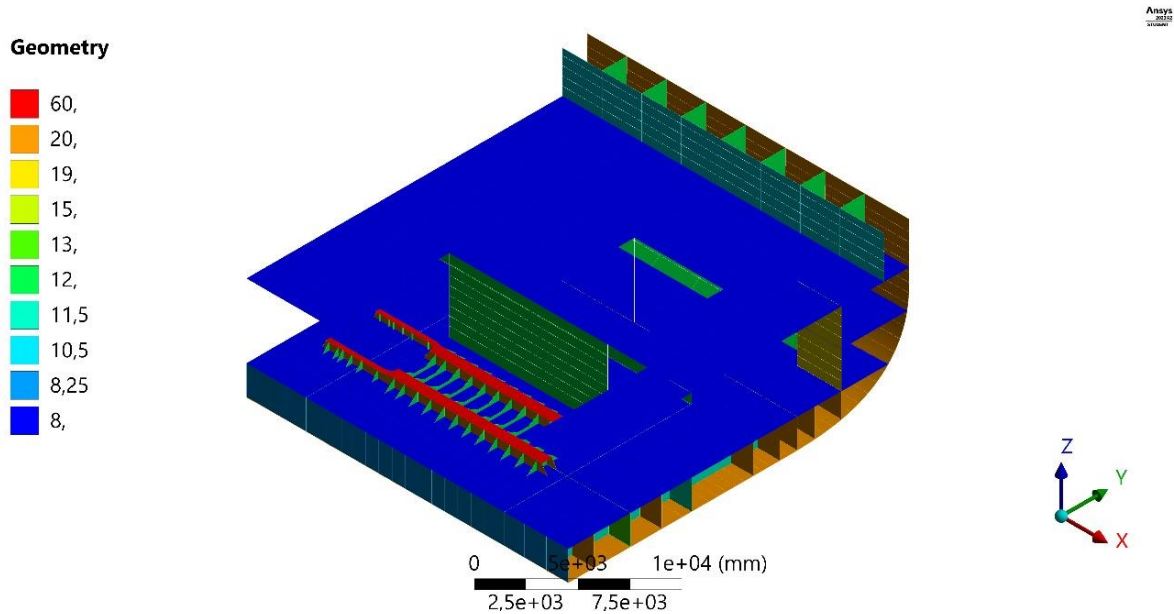


Figure 8. Thicknesses of the shell elements.

Once this key parameter is set, the mesh size of the finite element model must be established. To do that, a small simulation is performed to study the influence of the number of elements in the bending wavelength. In particular, a modal analysis (Fig. 9) of a simply supported beam made up of shell elements is done. The beam under analysis has a length of 5000 mm, a width of 100 mm and a thickness of 10 mm. The material assigned to the beam is structural steel. To validate the results of the finite element model, the first four natural frequencies are calculated as follows:

$$f_n = \frac{1}{2 \cdot \pi} \cdot \left[\frac{n \cdot \pi}{L} \right]^2 \cdot \sqrt{\frac{E \cdot I}{\rho}}, n = 1, 2, 3, \dots \quad (34)$$

Where:

n	=	beam mode
L	=	beam length, in m

E = Young's modulus, in Pa
 I = area moment of inertia, in m^4
 ρ = mass per unit of length, in kg/m.

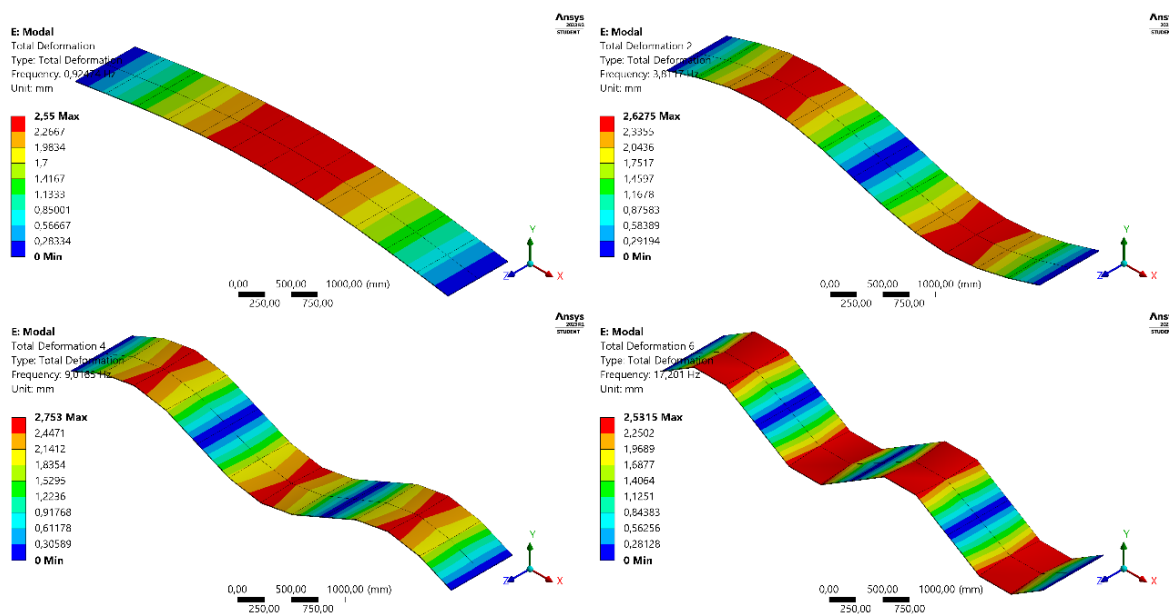


Figure 9. Modal analysis simply supported beam.

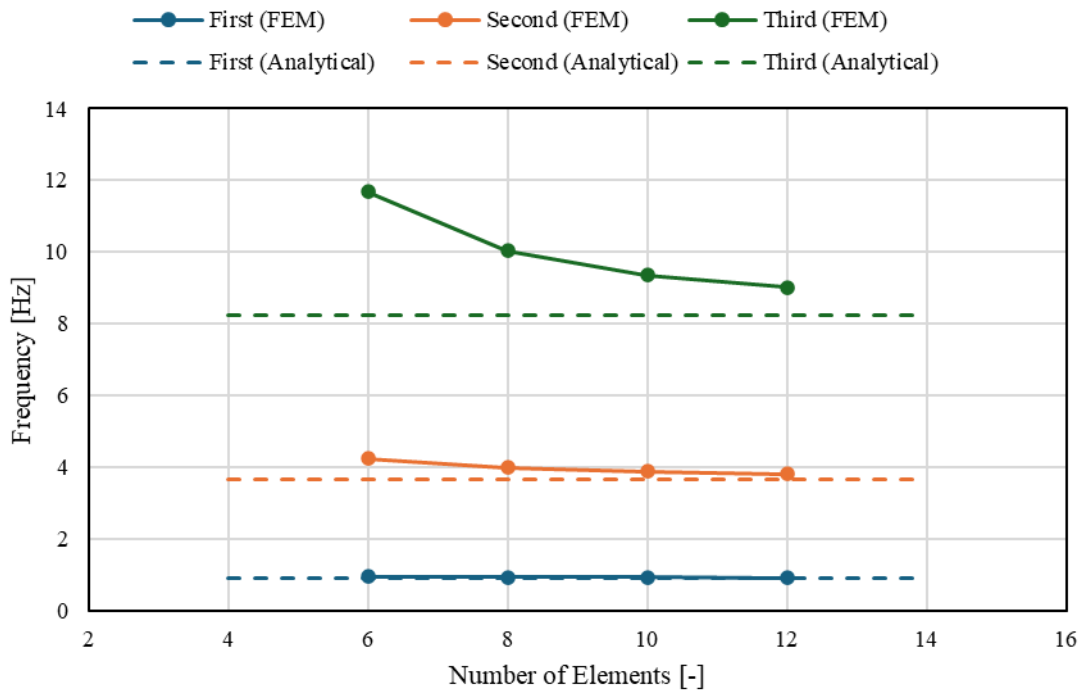


Figure 10. Modal analysis convergence plot.

The results from the finite element method and the analytical formulation are illustrated in Figure 10. Clearly, the difference between the analytical values and the finite element results increases as the frequency increases. From the beginning of the chapter, it is known that the bending wavelength decreases when the frequency increases. So, for a simulation with a given number of elements, the accuracy at higher frequencies is lost due to the element size is not small enough to represent the bending wavelength. To determine the element size, it is of interest to investigate the number of elements per bending wavelength at each frequency. The first mode of vibration only has the half of the wavelength. Therefore, to compare between the different frequencies, the number of elements per half wavelength (N) is shown:

Table 2. Influence of the number of elements per half wavelength on accuracy.

Frequency	N [-]	Error [%]
1 st	12,00	1,01
2 nd	6,00	4,09
3 rd	4,00	9,43
4 th	3,00	17,43

The latest results give an overview of the influence of mesh size (s) on accuracy. To ensure good accuracy, an error below five percent is assumed to be reasonable. Therefore, at least six elements per half wavelength are needed which results in a mesh size of 27,5 mm.

$$s = \frac{(\lambda/2)}{6} = \frac{\lambda}{12} \quad (35)$$

Despite the fact that the meshing criteria shown above is correct, it is not feasible to apply it because the computational cost is too high. So, in order to proceed with the calculations, three elements per half wavelength are considered. It is true that the error in this case is above the fifteen percent. In spite of everything, this is not a problem as the main objective of the analysis is to investigate the transmission losses between different parts of the ship structure. Since the transmission loss is the difference between two points of the structure, the error is present in both points and is cancelled. As a result, a compromise between the computational cost and accuracy is needed and the mesh size is fixed in 55 mm. (Wittekind, 2024)

This mesh of the structural model is composed of 2D elements such as triangular (Tri3) and quadratic (Quad4). The majority of elements in the mesh are quadratic while triangular elements are only used when the mesh requires a transition. (ANSYS4, 2017)

After applying the meshing criteria to the structural model, with a mesh size of 55 mm, the mesh has $7,57E+05$ elements. The discretization at the location of the foundation is shown in Figure 11.

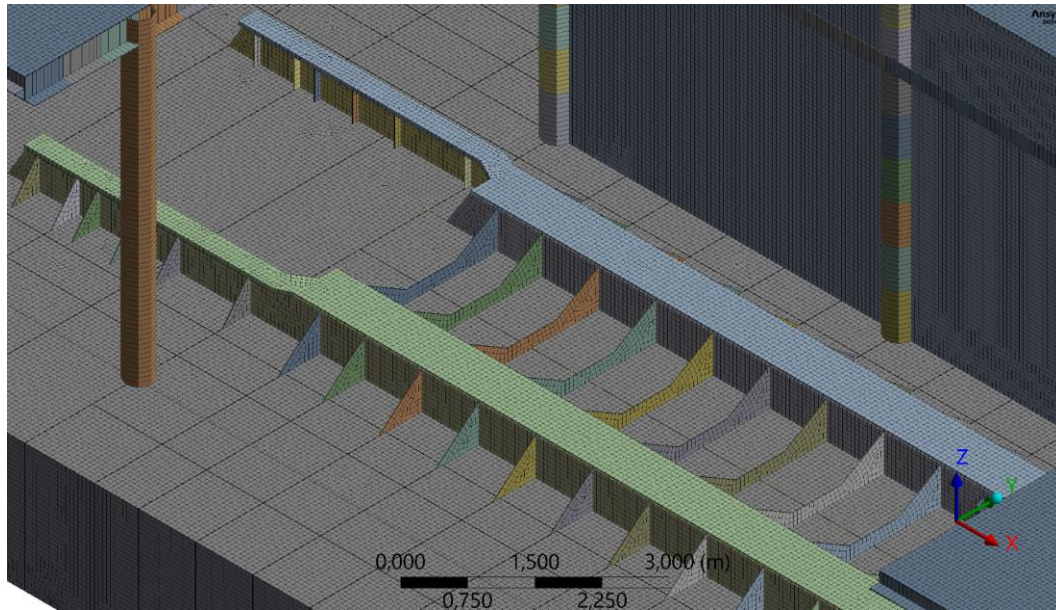


Figure 11. Mesh at the engine foundation.

The quality of the mesh can be quantified in several ways. The FEM software performs several geometrical checks on mesh elements in order to determine their quality. These checks, or metrics are (MECHEAD, 2023):

- Element quality.
- Aspect ratio calculation.
- Jacobian ratio.
- Warping factor.
- Parallel deviation.
- Maximum corner angle.
- Skewness.
- Orthogonal quality.

All the mesh metrics mentioned above are checked to see that the mesh model has good quality (Fig. 12).





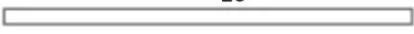




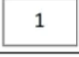
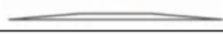
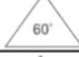

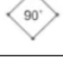
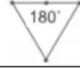
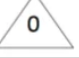

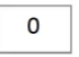

Metric	Best		Worst
Element Quality	1		0
Aspect Ratio - Triangle	1 		20 
Aspect Ratio - Quadrilaterals	1 		20 
Jacobian Ratio	1	10	
Warping Factor - Shell	0 		5 
Warping Factor - Brick	0 		0.4 
Parallel Deviation	1 		170 
Maximum Corner Angle - Triangular	60° 		165° 
Maximum Corner Angle - Quadrilateral	90° 		180° 
Skewness - Triangular	0 		1 
Skewness - Quadrilateral	0 		1 
Orthogonal Quality	1		0

Figure 12. Mesh metrics. Available from

<https://www.mechead.com/mesh-quality-checking-ansys-workbench/>

[Accessed 19 July 2024].

2.3.4 Loading Cases

Firstly, the boundary conditions in the structure are defined. Fixed supports are applied in the boundaries of the model and the symmetry condition is applied in the geometry located in the centre line. For an engine with four mounts, the structure should be excited with 4 forces. But it is preferable to have one force of 1 Newton and four loading cases, to directly read velocity levels. So, the resultant case will be the average of the four loading cases. Finally, the structural damping is set at 3%. (Wittekind, 2024)

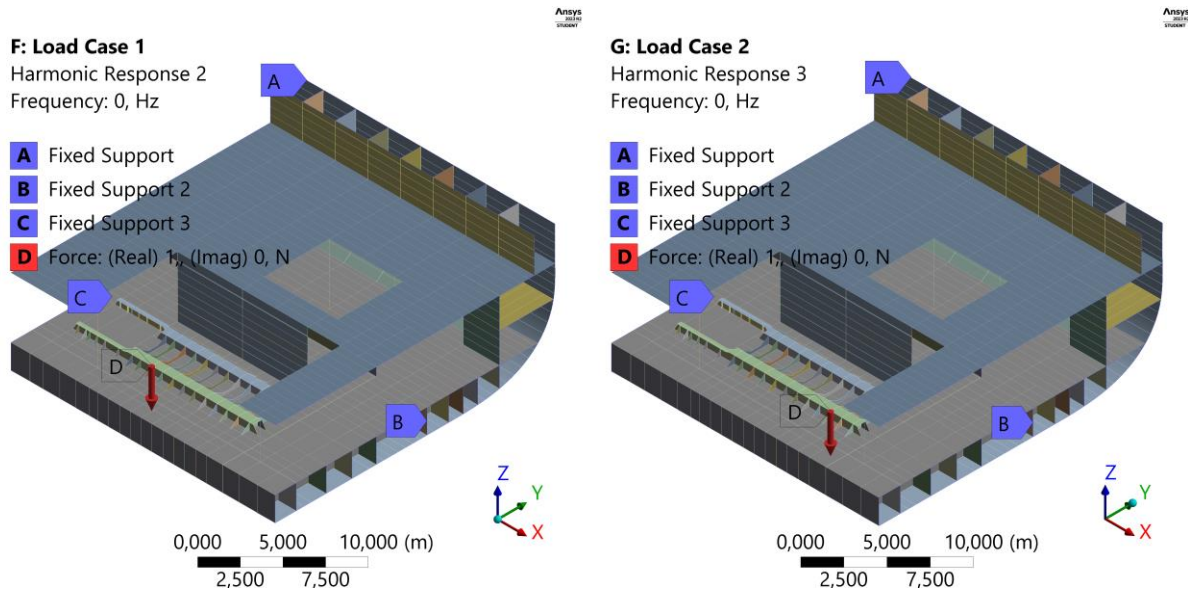


Figure 13. Loading cases 1 and 2.

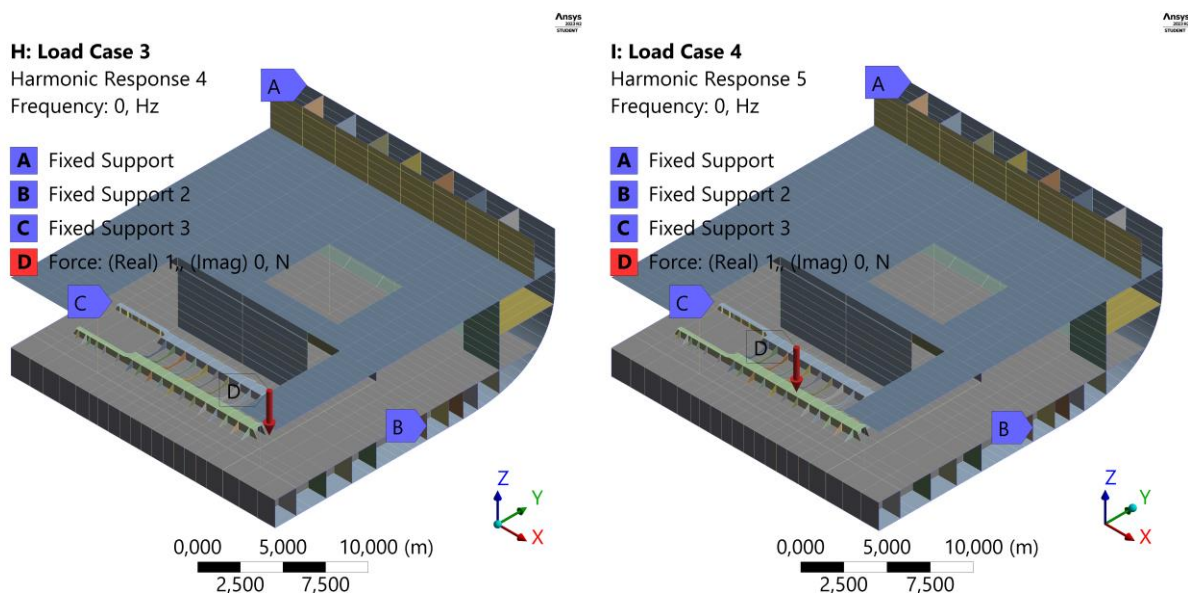


Figure 14. Loading cases 3 and 4.

2.3.5 Calculation Points

To perform the analysis, the transmission losses between different points of the structure are needed. The following areas are defined:

- Foundation.
- Effective source area.
- Deck (top).
- Deck (side).

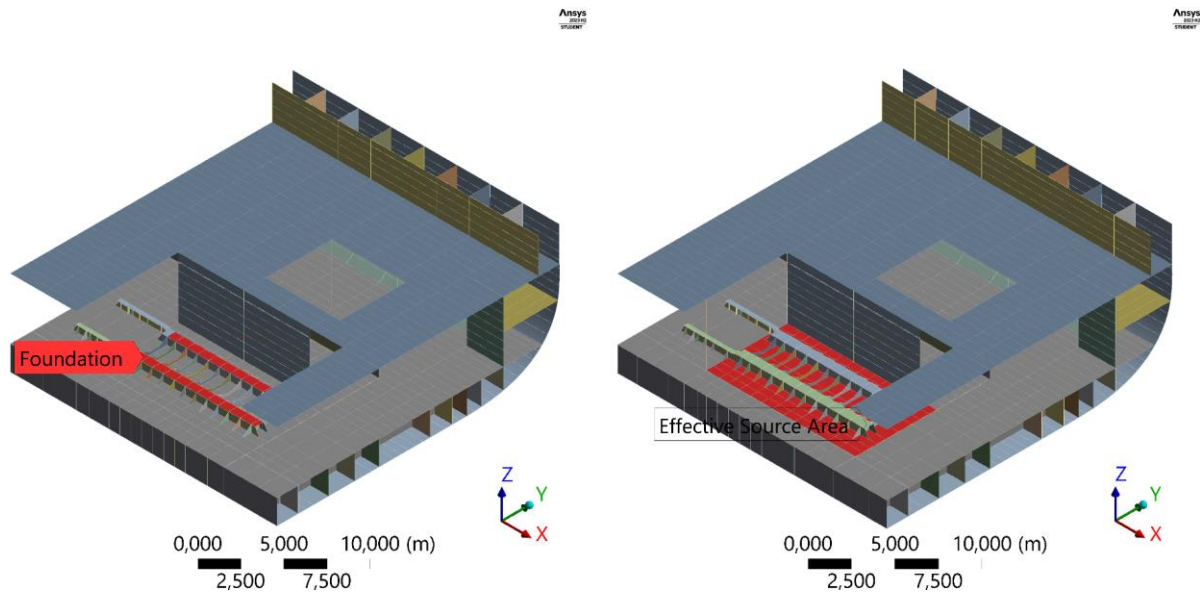


Figure 15. Location of the foundation and the effective source area.

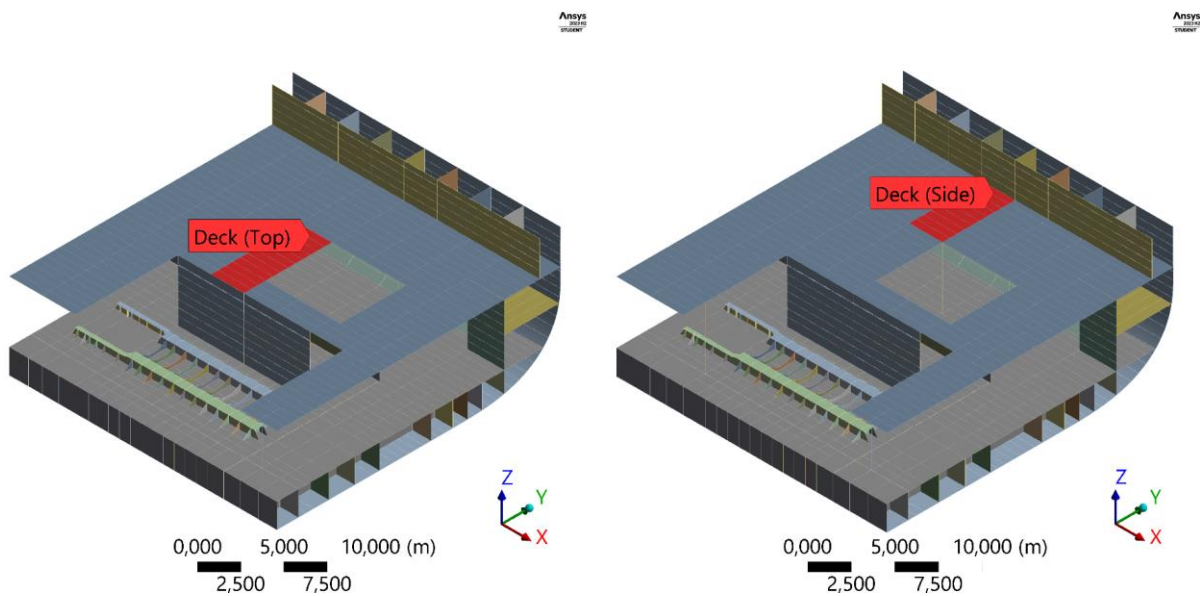


Figure 16. Location of the deck (top) and deck (side).

Additionally, to study how changes in the engine foundation influence the structure-borne noise propagation, four points are defined to read the results in the different load cases. The location of the points (Fig. 17) is chosen in such a way that it matches the application point of the forces in the different loading cases. By looking the differences in the response between these points a methodology will be defined (Section 3.2) to estimate how the noise is reduced or amplified when changes in the foundation are made. As it was mentioned before, the engine suppliers give the structure-borne noise at the top of the engine foundation for the test foundation. So, it is of big interest to study how this noise is modified when the engine is placed in the real foundation to determine limit conditions in shipboard machinery installation.

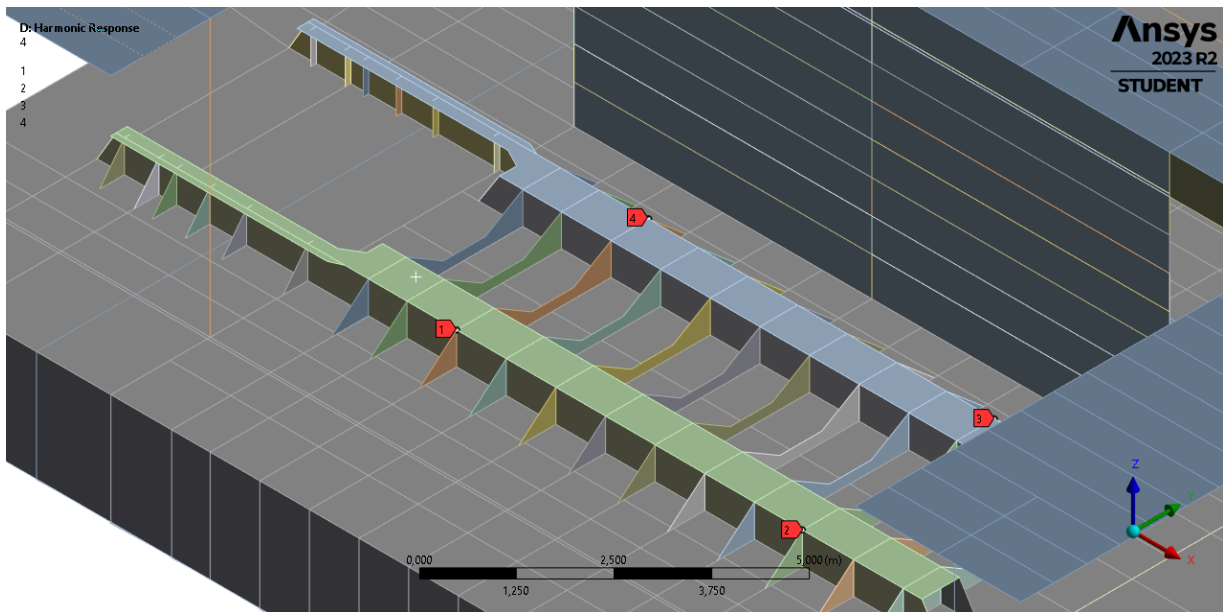


Figure 17. Location of the calculation points on the foundation.

3. RESULTS

3.1 Transmission Losses Calculation

In this section, the transfer functions or transmission losses between the different points of the structure are determined. First, the harmonic analysis is performed and the frequency response function at each part of the structure is obtained (Fig. 18-24-27). Secondly, the transmission losses are determined according to Eq. 2 (Fig. 19-25-28). Additionally, the response of the structure for different frequencies is shown (Fig. 20-21-22-23-26-29) to identify frequency ranges where resonance phenomena could occur. Finally, the results from SNAME and the FEM are compared to identify the limitations of the empirical method proposed by SNAME.

3.1.1 From Foundation to Effective Source Area

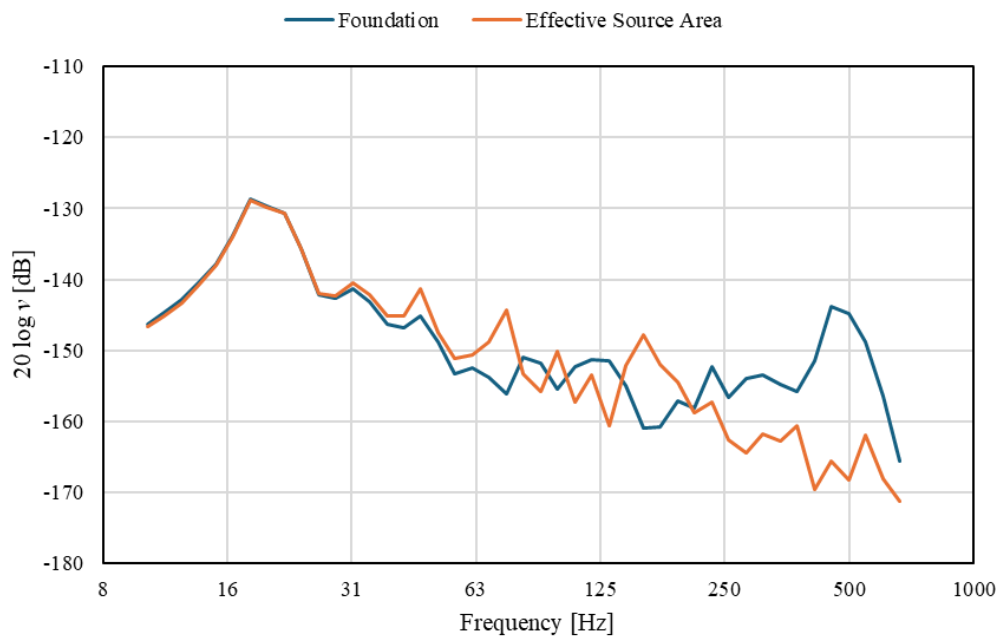


Figure 18. Frequency response function: foundation and effective source area.

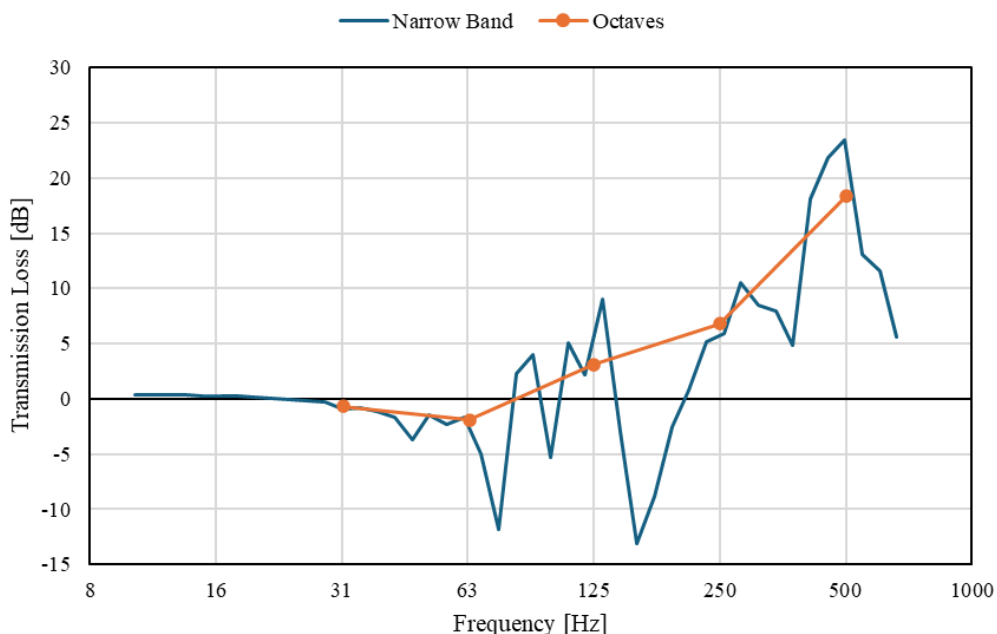


Figure 19. Transmission losses from foundation to effective source area.

The frequency response function (Fig. 18) presents two different regions. One region where the response in the effective source area is amplified (Fig. 20-21) which is the expected result according to SNAME. In the other region, especially for the octave bands of 250 Hz and 500 Hz (Fig. 19), the response from the foundation top to the effective source area is attenuated.

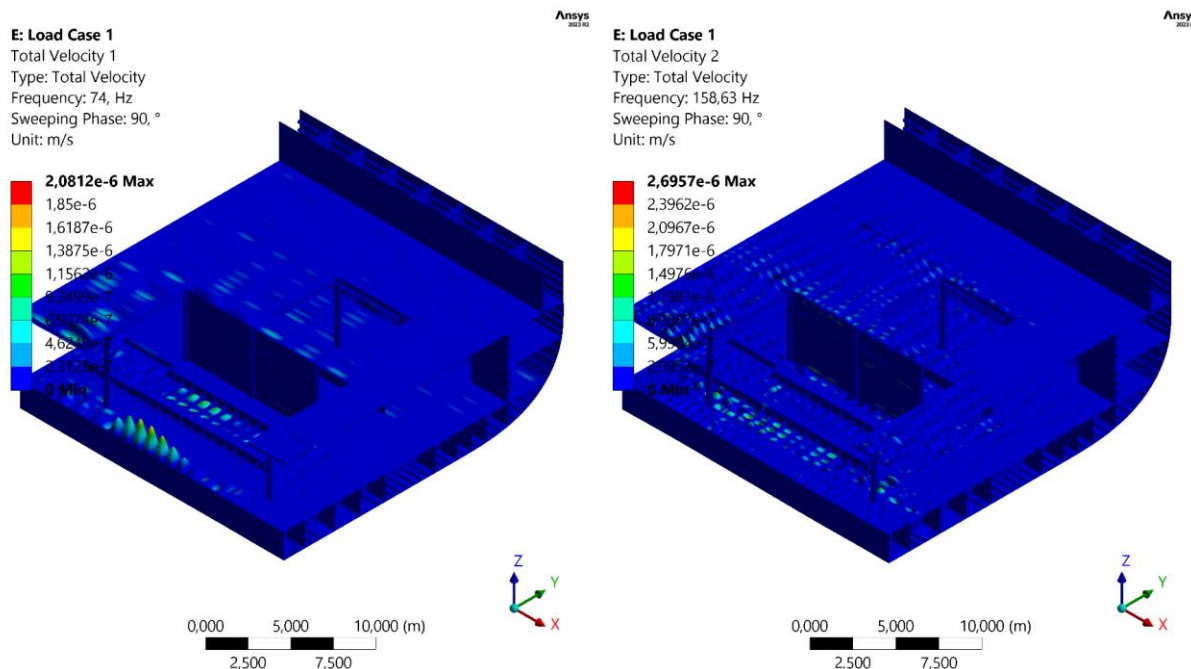


Figure 20. Response of the structure at 74 Hz and 158,6 Hz.

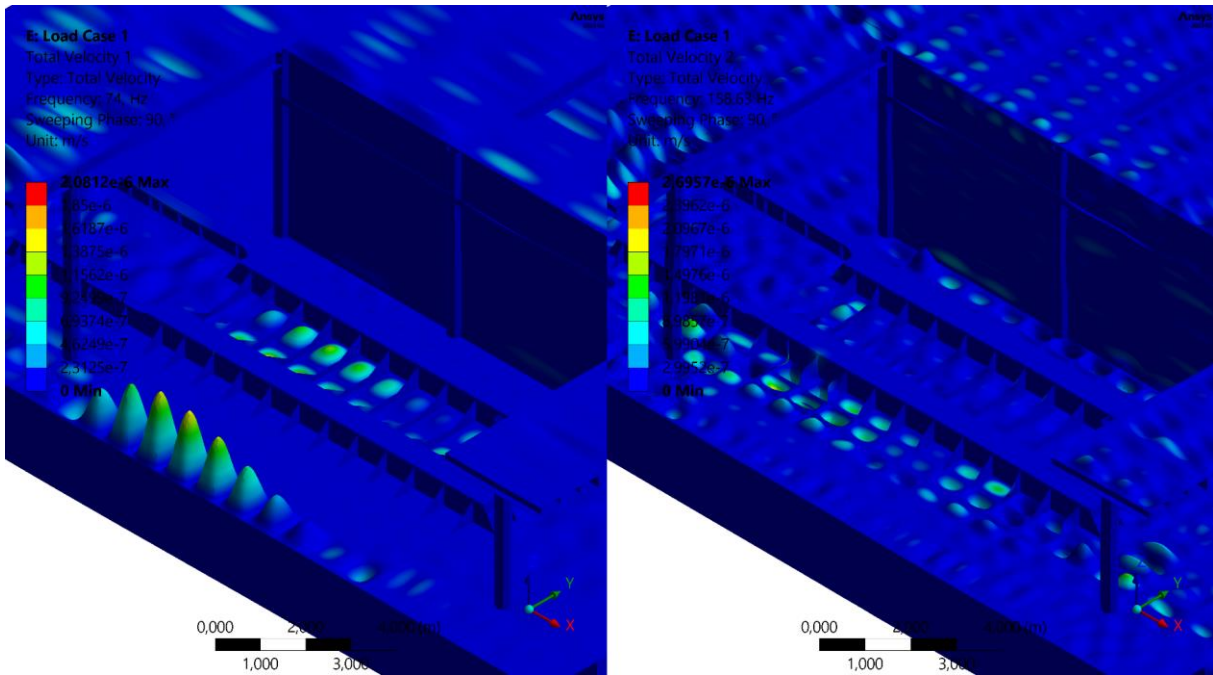


Figure 21. Response at the location of the foundation at 74 Hz and 158,6 Hz.

The peaks of the foundation response (Fig. 18) at high frequencies indicate high amplitudes in the response (Fig. 22-23) while the response in the effective source area is significantly lower which results in positive transmission losses which means a reduction of noise. According to Figure 19, the reduction of noise for the octaves band of 250 Hz is of 7 dB and for the octave band of 500 Hz the reduction is of 18 dB.

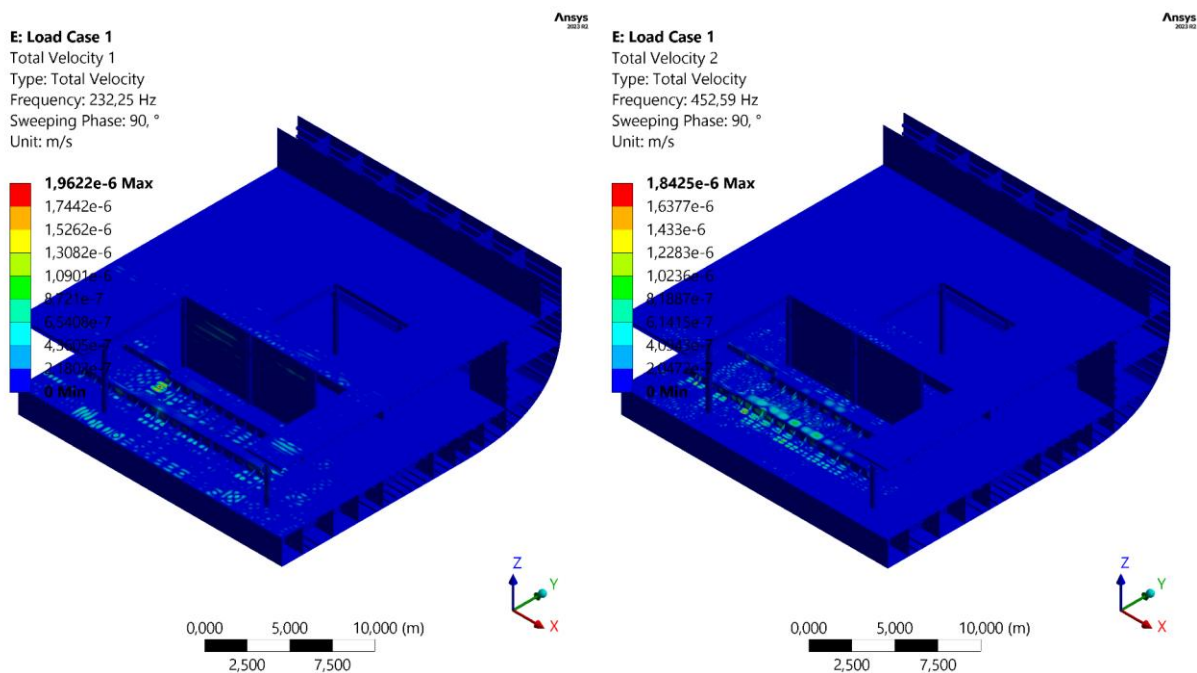


Figure 22. Response of the structure at 232,2 Hz and 452,6 Hz.

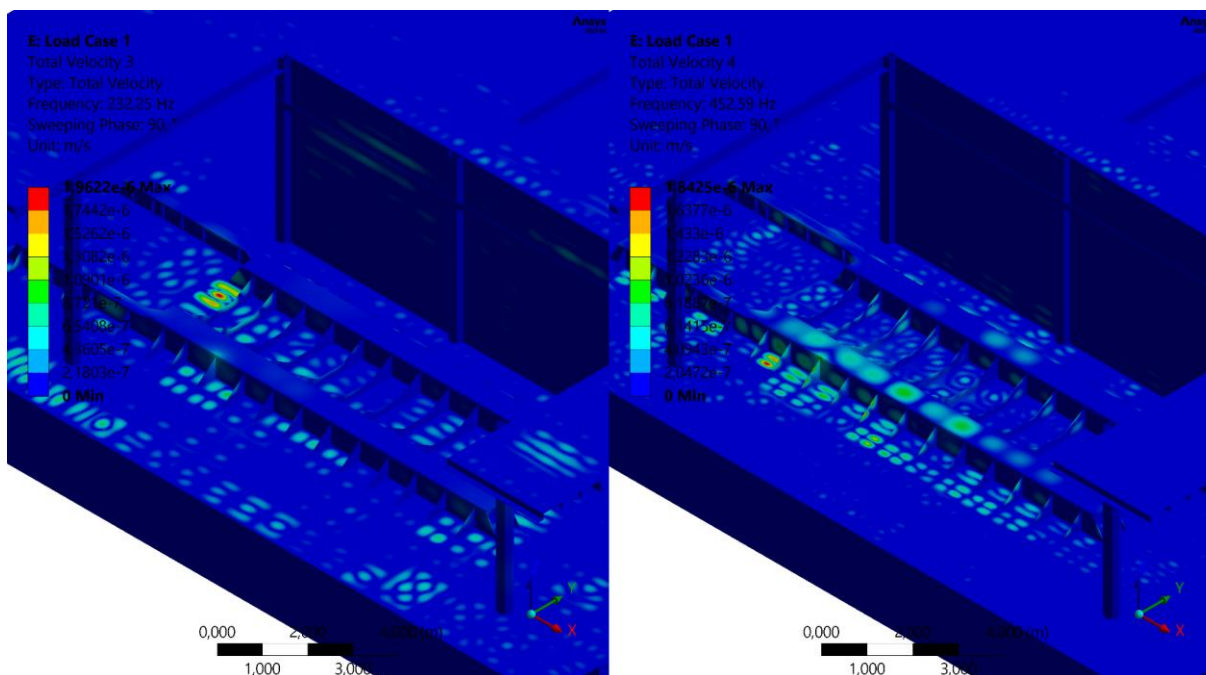


Figure 23. Response at the location of the foundation at 232,2 Hz and 452,6 Hz.

3.1.2 From Effective Source Area to Deck (Top)

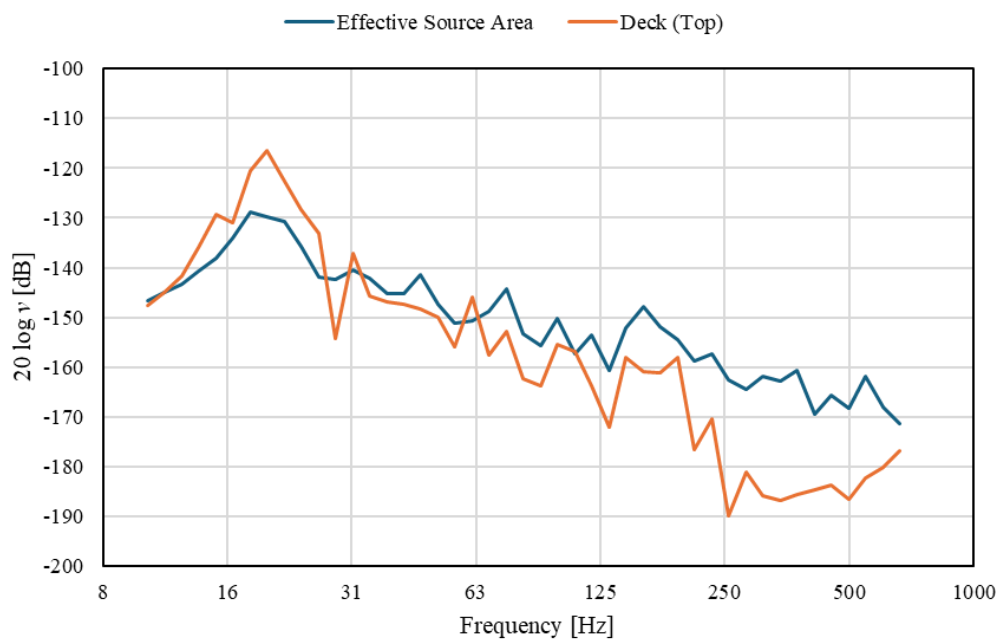


Figure 24. Frequency response function: effective source area and deck (top).

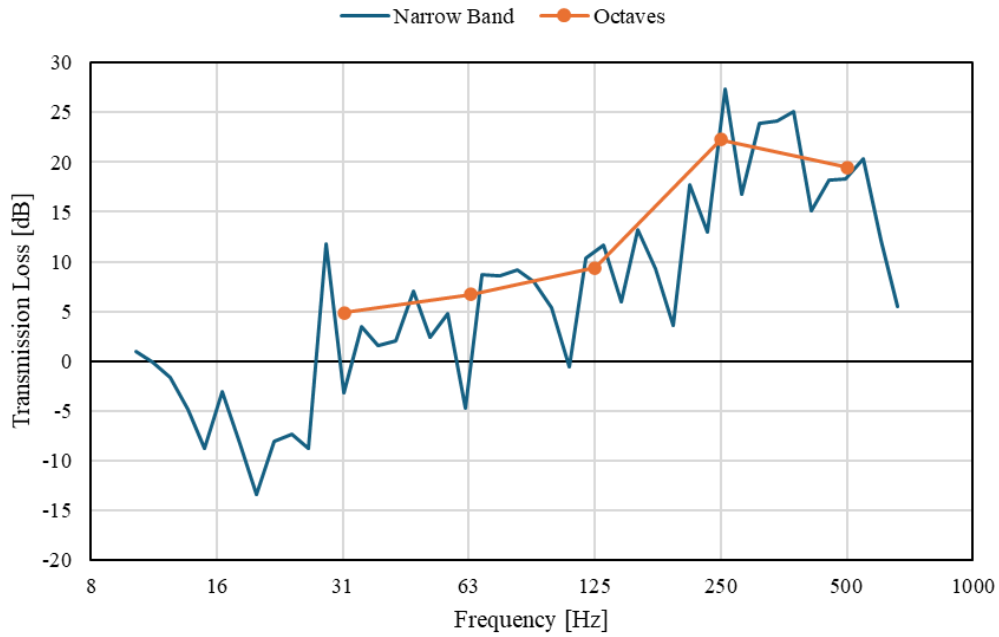


Figure 25. Transmission losses from effective source area to deck (top).

The results from this area (Fig. 24-25) are as expected, since the noise from the effective source area to the deck (top) is reduced for all the octave bands. It is true that for the lower frequencies the noise is amplified due to for these frequencies there is a resonance phenomenon present (Fig. 26) which should be avoided.

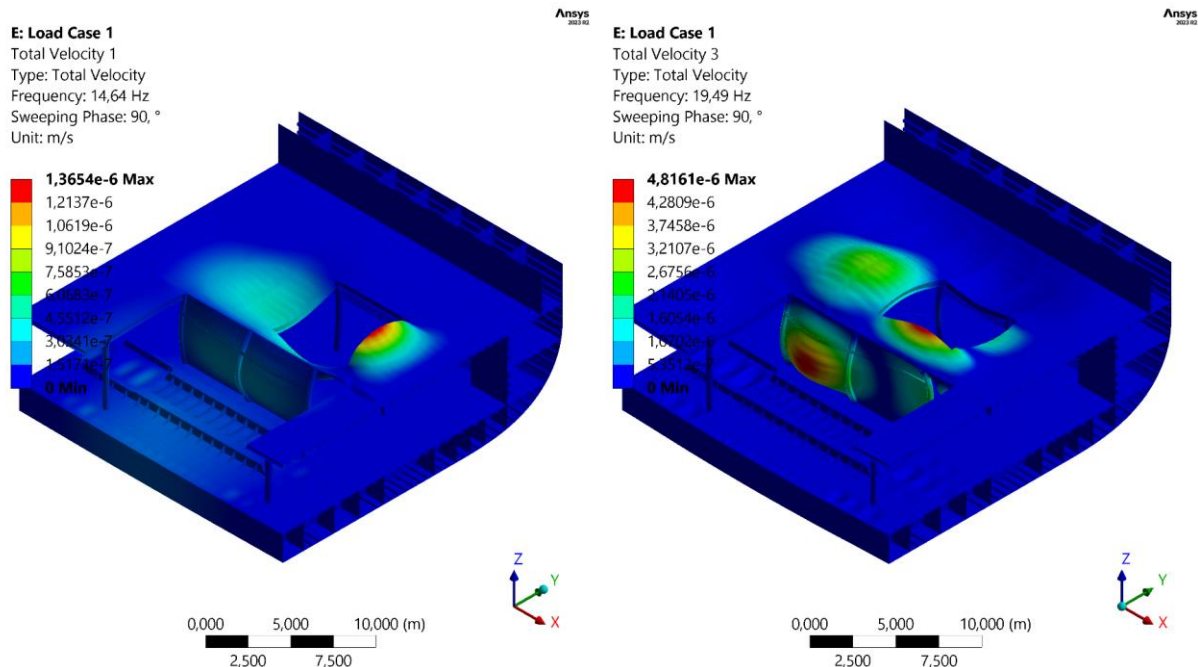


Figure 26. Response of the structure at 14,6 Hz and 19,5 Hz.

3.1.3 From Effective Source Area to Deck (Side)

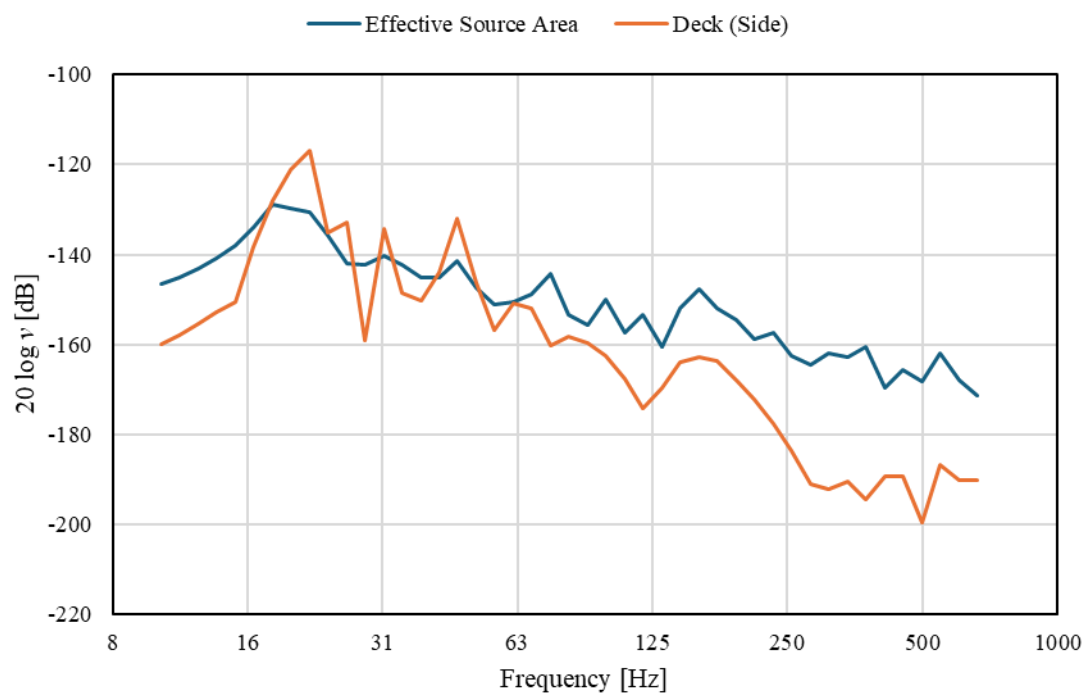


Figure 27. Frequency response function: effective source area and deck (side).

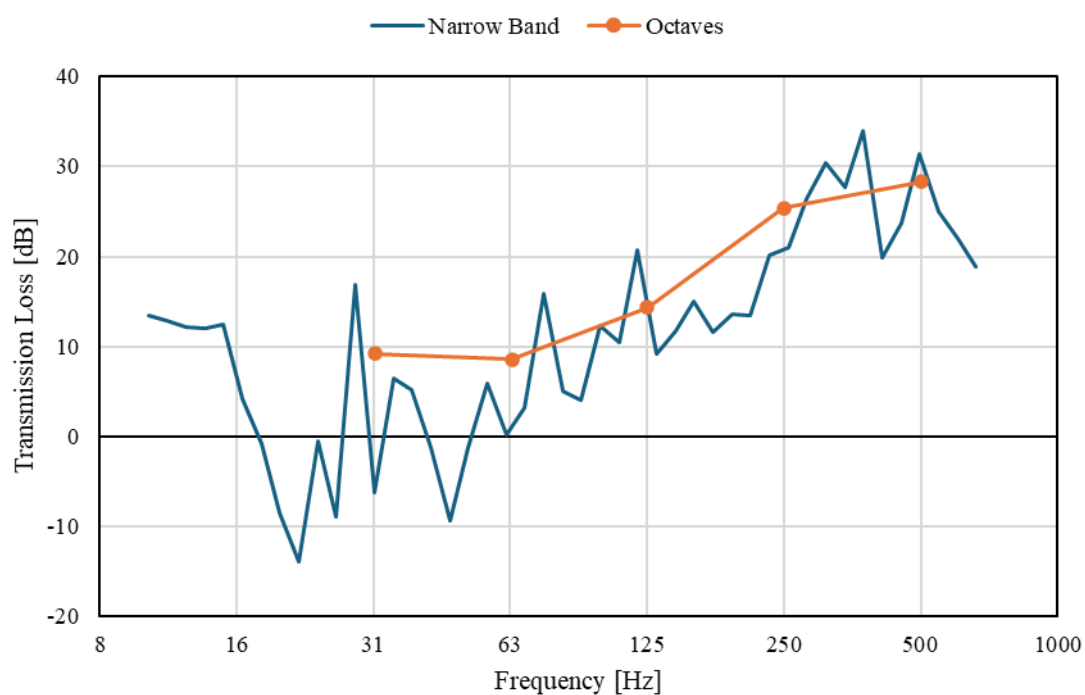


Figure 28. Transmission losses from effective source area to deck (side).

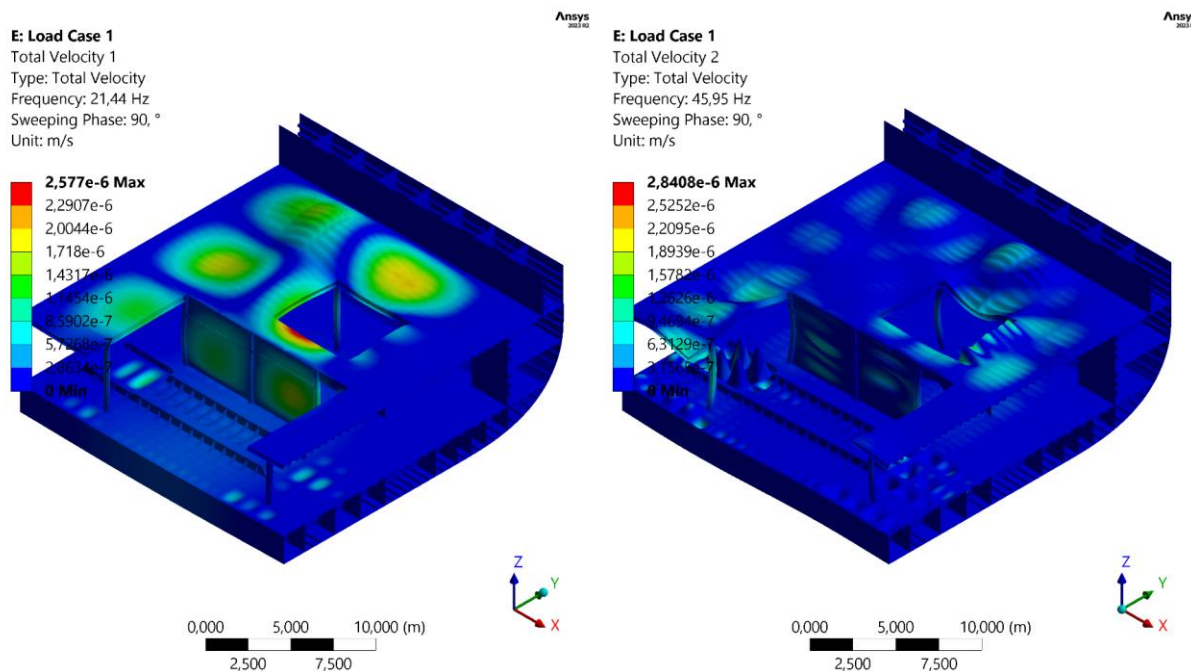


Figure 29. Response of the structure at 21,4 Hz and 45,9 Hz.

The results from this area (Fig. 27-28) are as expected, since the noise from the effective source area to the deck (side) is reduced for all the octave bands. These results allow to understand how the noise transmission occurs. Starting from the excitation point, the structure-borne noise travels from the effective source area to the deck above, at that point, a reduction of noise is produced due to the intersection of the bulkhead with the two decks. Then, the structure-borne noise is reduced as it moves far from the noise source.

3.1.4 Comparison SNAME and FEM

Once the transmission losses between the different points of the structure are determined, the airborne noise can be obtained at any area of the structure. Only the structure-borne noise at the foundation top is needed which is given by DW-ShipConsult:

Table 3. Vibration velocity levels on the foundation top.

Freq. (Hz)	31,5	63	125	250	500
L_v (dB)	74	71	74	80	75

After applying the transmission losses, the radiation efficiency and A-weighting filtering (Section 2.1) the airborne noise on deck (top) is shown in Figure 30.

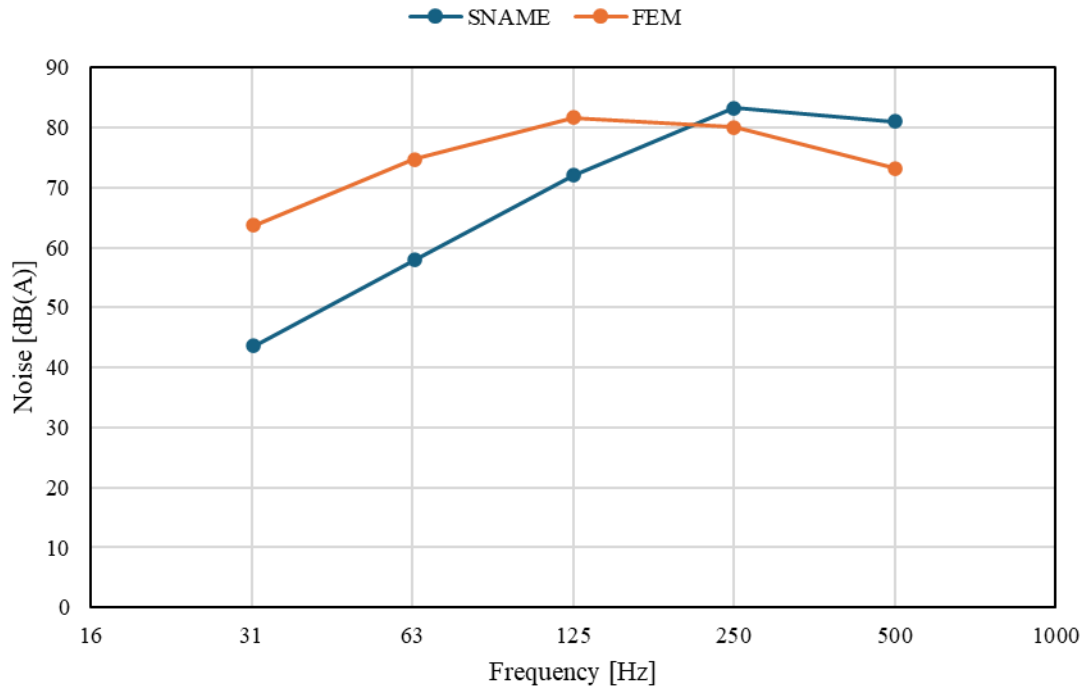


Figure 30. Airborne noise on deck (top) according to SNAME and FEM.

The obtained results show that the results from SNAME and the FEM are very close for the octave bands above 125 Hz. However, for the octave band of 125 Hz and below there is a big difference between the empirical method and the numerical analysis. These results highlight the limitations of the empirical method when the analysis is performed for the octave bands below 125 Hz where the data from high frequency is extrapolated.

3.2 Limit Conditions in Shipboard Machinery Installation

As it was mentioned before, it is of interest to determine how the noise is amplified or reduced when changes in the machinery foundation are made. This is a common issue for designers since engine suppliers specify the structure-borne noise on the top of the test foundation. But designers are not interested in this value since the engine foundation on the ship has not the same characteristics and hence the noise will be different which could cause a violation of limit conditions in shipboard machinery installation. To determine how changes in the foundation modify the noise, the geometry of the engine foundation will be modified (Fig. 30). In particular, a reduction of the scantlings is done which will result in an amplification of the noise.

Table 4. Reduction of scantling in the engine foundation.

Foundation	Thickness 1 [mm]	Thickness 2 [mm]	Thickness 3 [mm]
Strong	60	20	12
Weak	20	10	8

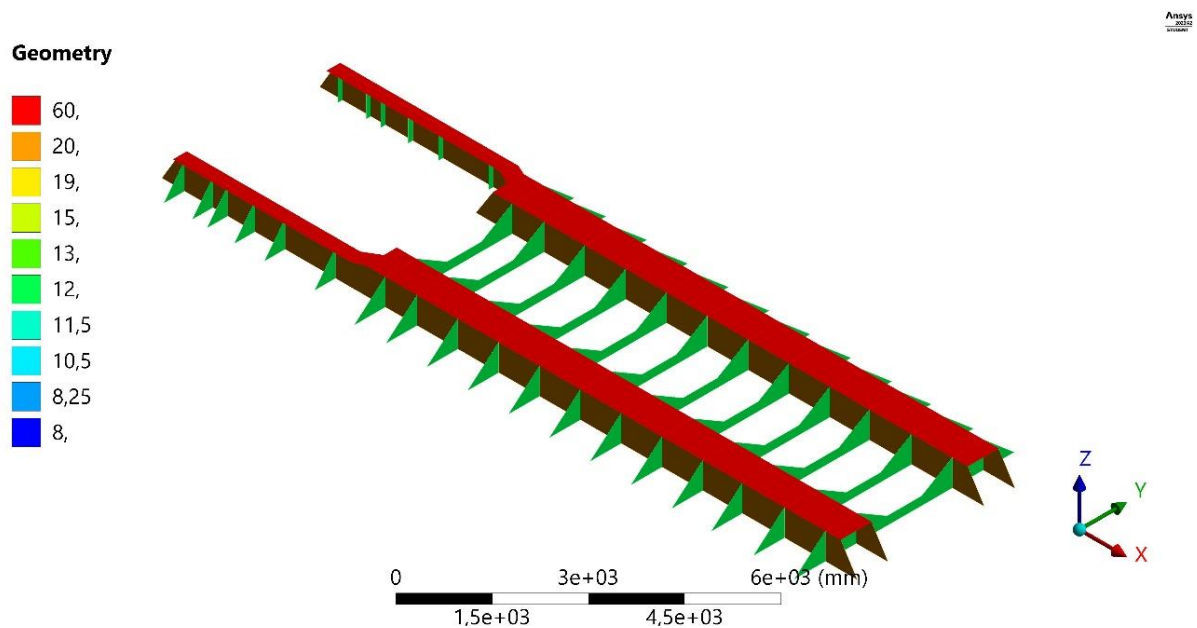


Figure 31. Engine foundation initial geometry.

The methodology to determine the limit conditions in shipboard machinery installation is described here below:

- Response at the calculation points of the engine foundation.

- Transmission losses between the point where the force is applied and the rest of the points for the different load cases as shown in Fig. 32-36-39.

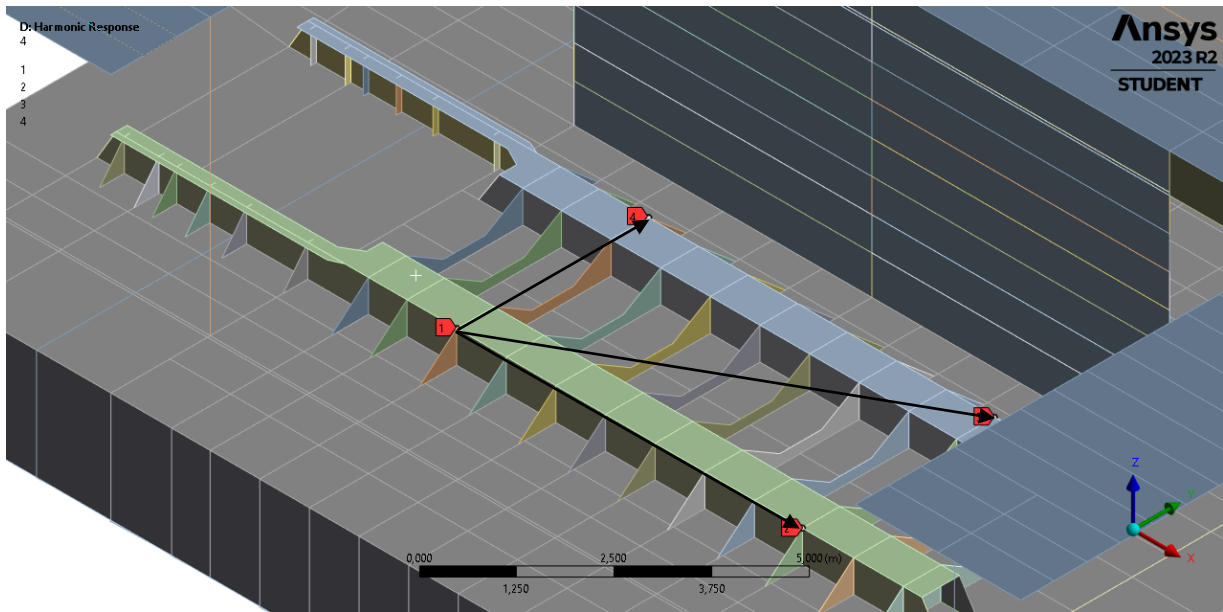


Figure 32. Calculation points for the first load case.

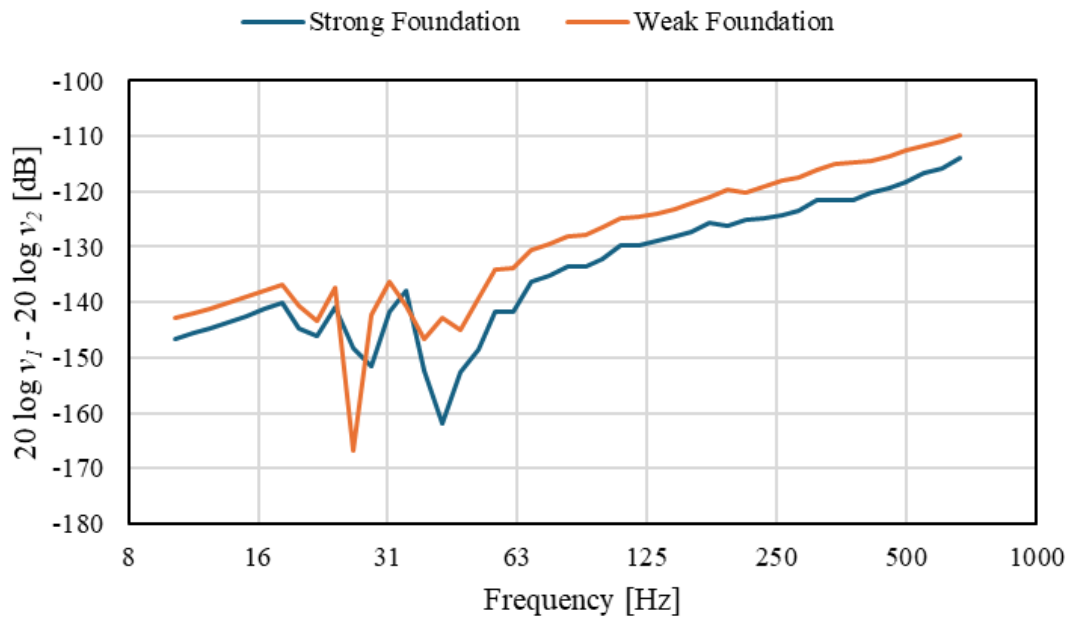


Figure 33. Transfer function between point 1 and 2.

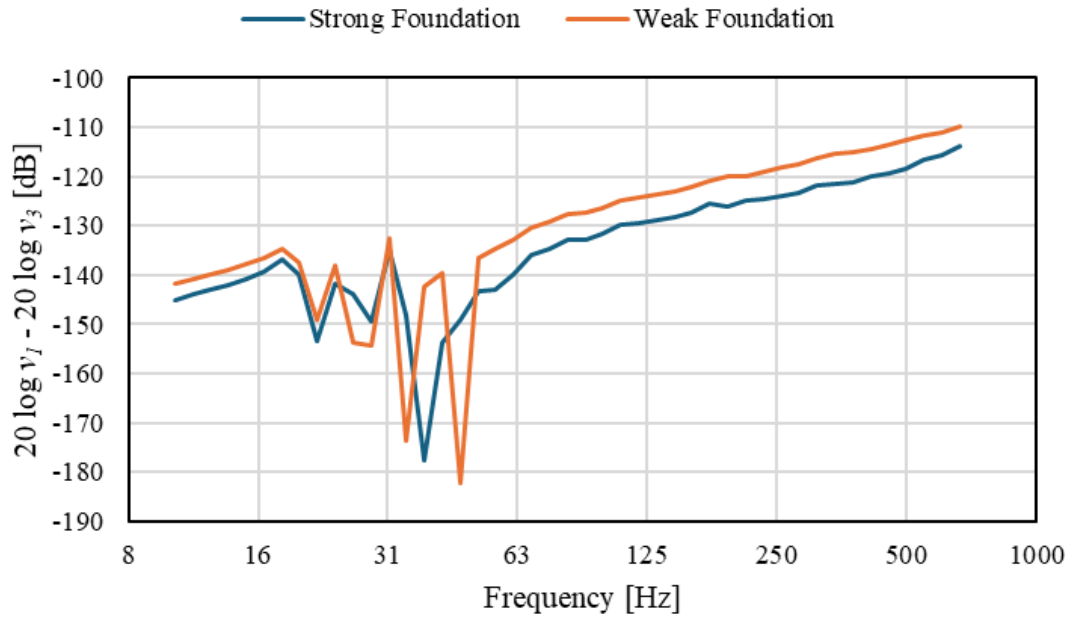


Figure 34. Transfer function between point 1 and 3.

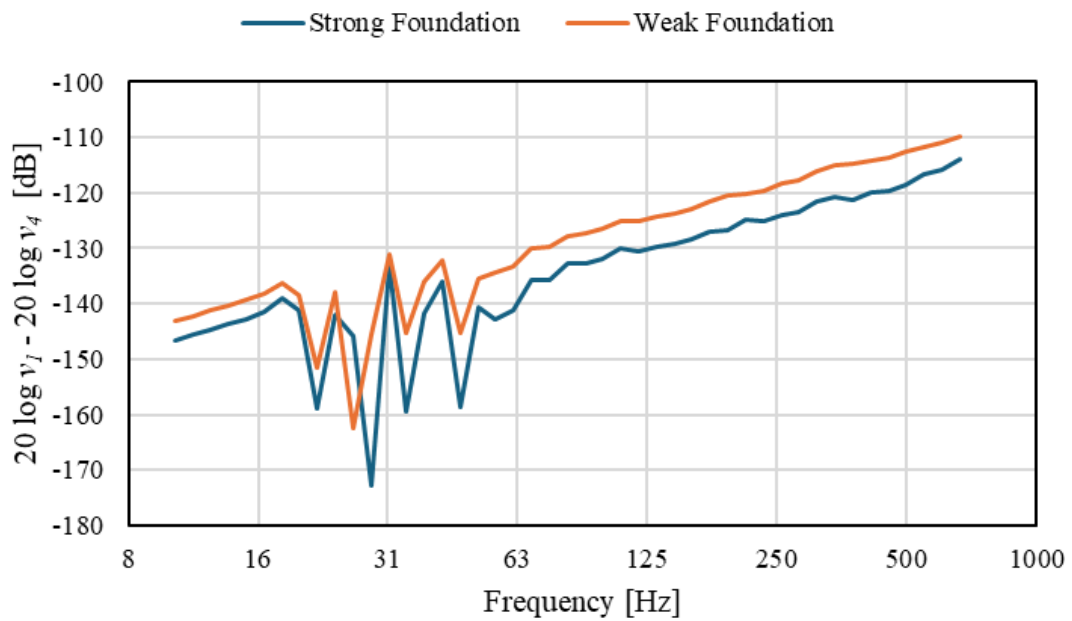


Figure 35. Transfer function between point 1 and 4.

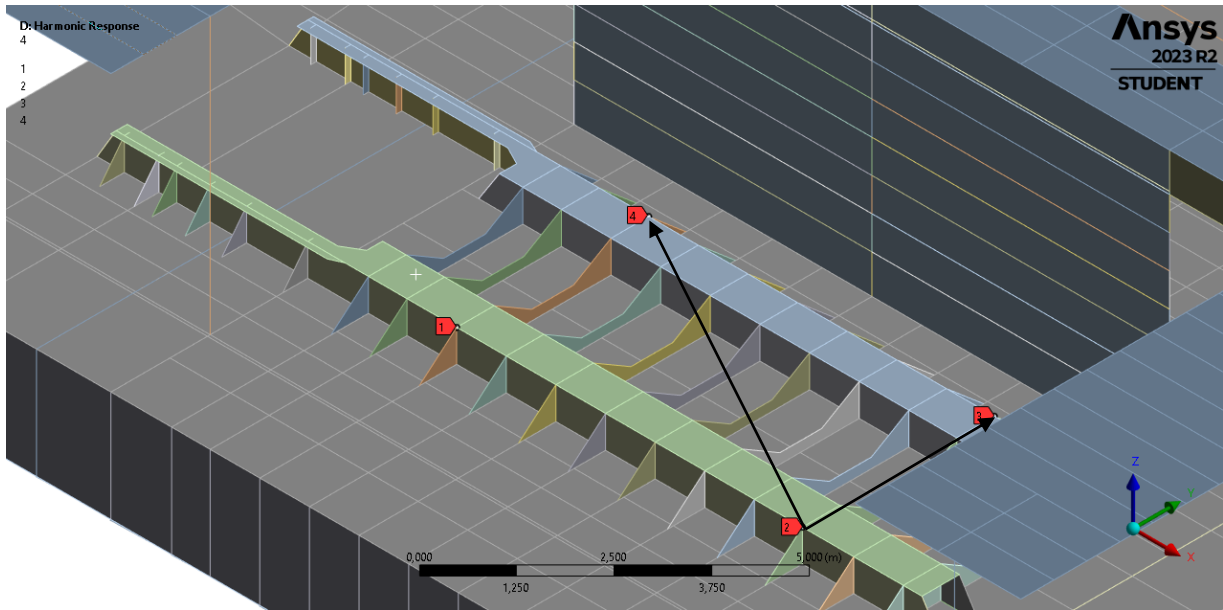


Figure 36. Calculation points for the second load case.

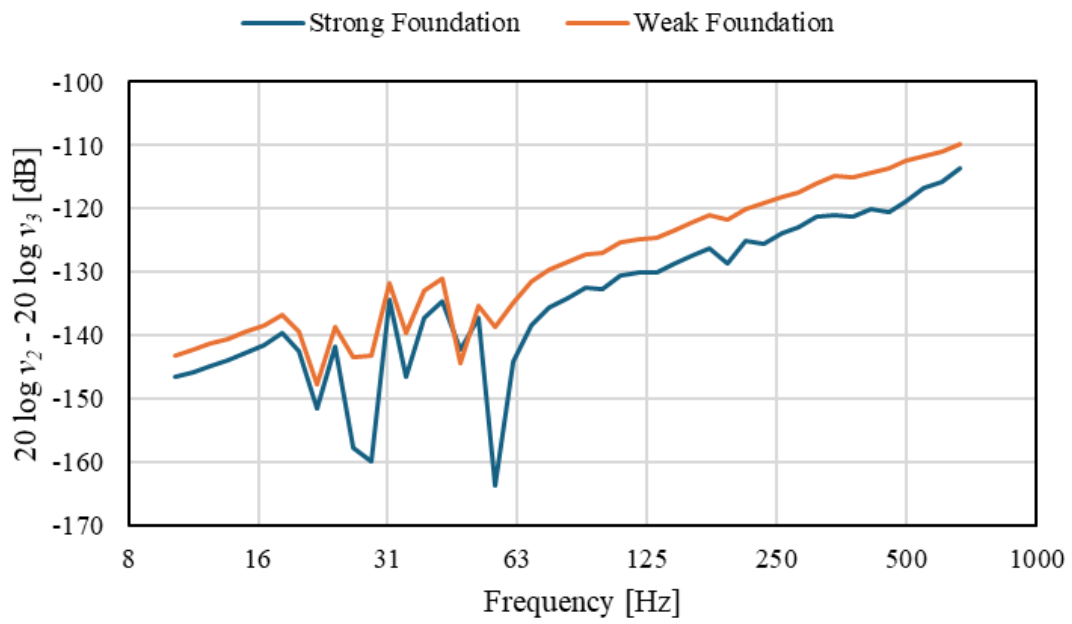


Figure 37. Transfer function between point 2 and 3.

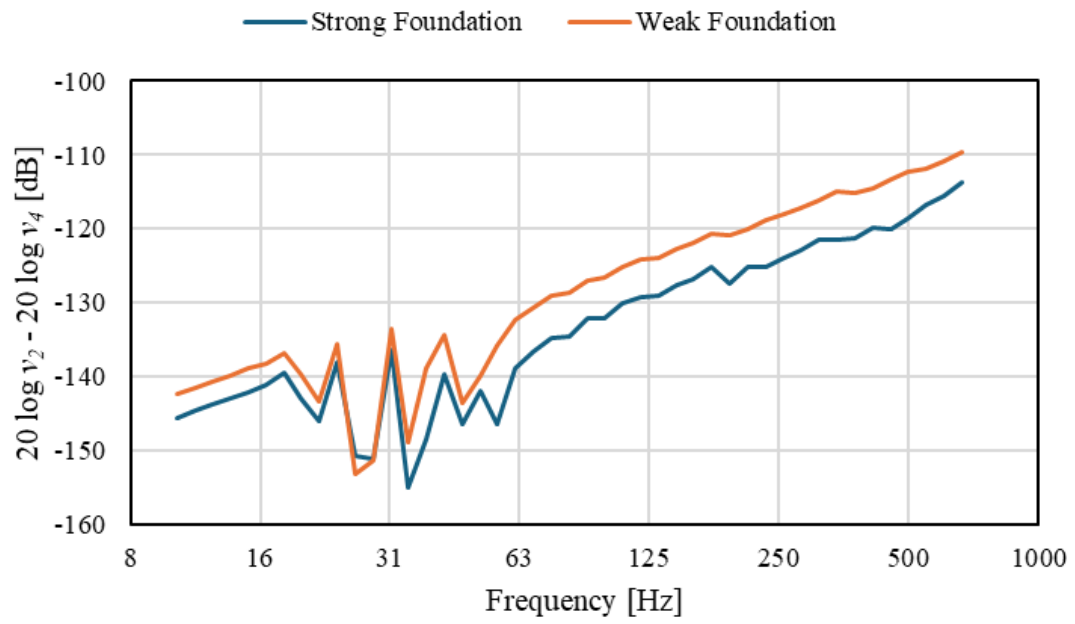


Figure 38. Transfer function between point 2 and 4.

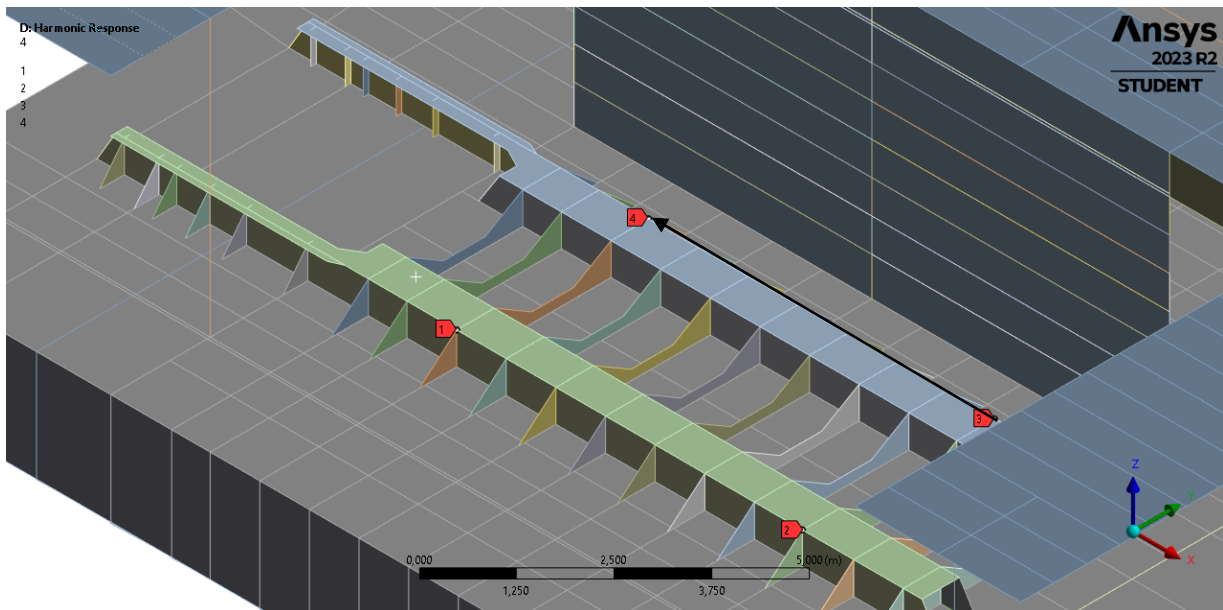


Figure 39. Calculation points for the third load case.

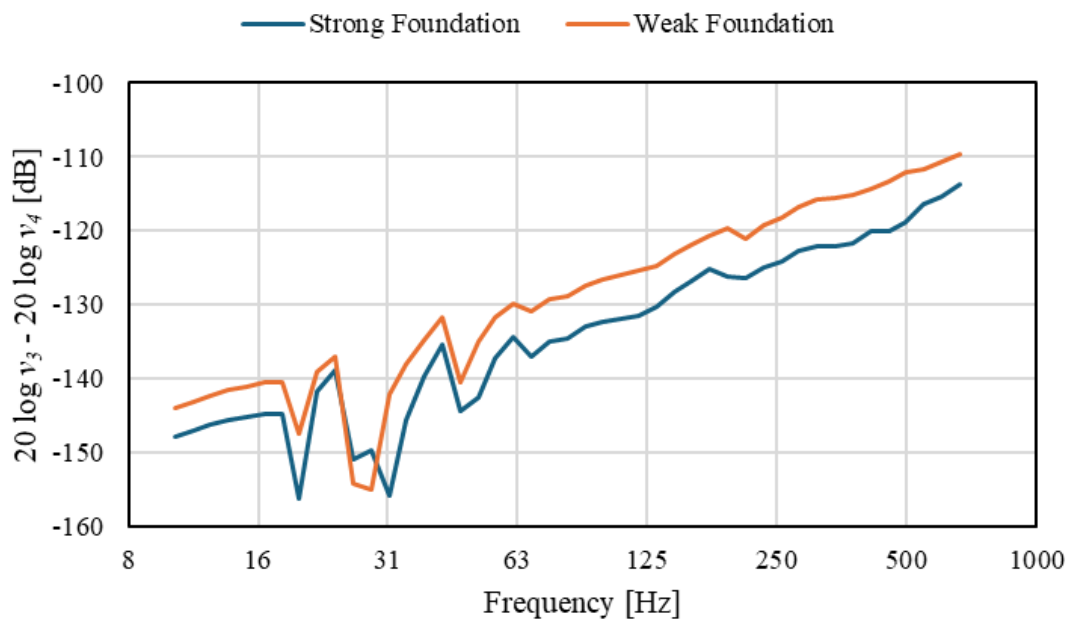


Figure 40. Transfer function between point 3 and 4.

- Average of the six transfer functions for each foundation. F subscripts for the points where the force is applied in the different loading cases. X subscripts for the points where the force is not applied in the different loading cases.

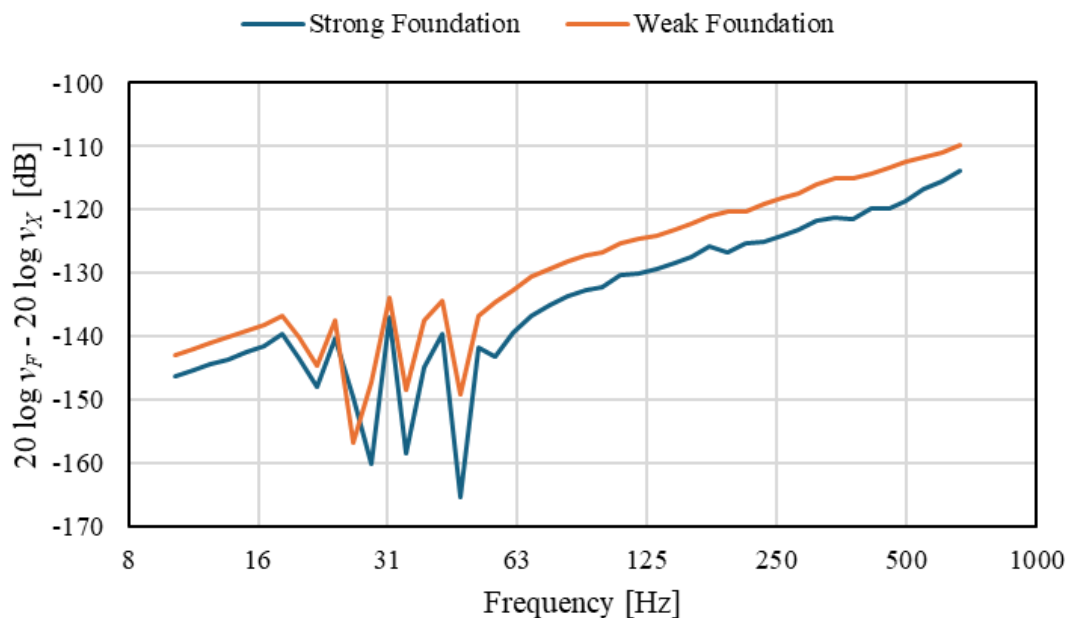


Figure 41. Average of the six transfer functions for both foundations.

- Different between the strong and weak foundation to obtain the increment of noise.

Table 5. Noise amplification.

Freq. (Hz)	31,5	63	125	250	500
ΔL_v (dB)	0,02	-6,7	-5,2	-5,8	-5,4

The values from Table 5 are added to the values from Table 3 to obtain the structure-borne noise on the top of the engine foundation. These values should be checked with the criteria to see if the new levels of noise satisfy the requirements.

Table 6. Vibration velocity levels on the foundation top for the weak foundation.

Freq. (Hz)	31,5	63	125	250	500
L_v (dB)	74	77,7	79,2	85,8	80,4

ABS provides a criterion for noise levels onboard vessels (Table 7). A-weighted sound pressure levels of the vessel need to be used for the comparison with the criteria. (ABS, 2019)

Table 7. Noise Level Limits, dB(A).

Designation of Rooms and Spaces	Ship Size	
	1600 up to 10000 GT	>10 000 GT
Workspaces		
Machinery spaces	110	110
Machinery control room	75	75
Workshops	85	85
Non-specified workspaces	85	85
Navigation Spaces		
Navigation bridge and chartrooms	65	65
Look-out-posts	70	70
Radio rooms	60	60
Radar rooms	65	65
Accommodation Spaces		
Cabin and hospitals	60	55
Messrooms	65	60
Recreation rooms	65	60
Open recreation areas	75	75
Offices	65	60

Service Spaces		
Galleys	75	75
Serveries and pantries	75	75
Normally unoccupied spaces	90	90

3.3 Comparison Between Foundations

Once the increment of noise on the top of the engine foundation has been determined. It is of interest to study if the change of geometry has influence in structure-borne propagation in other parts of the structure. To perform the analysis, the response at the following locations is studied:

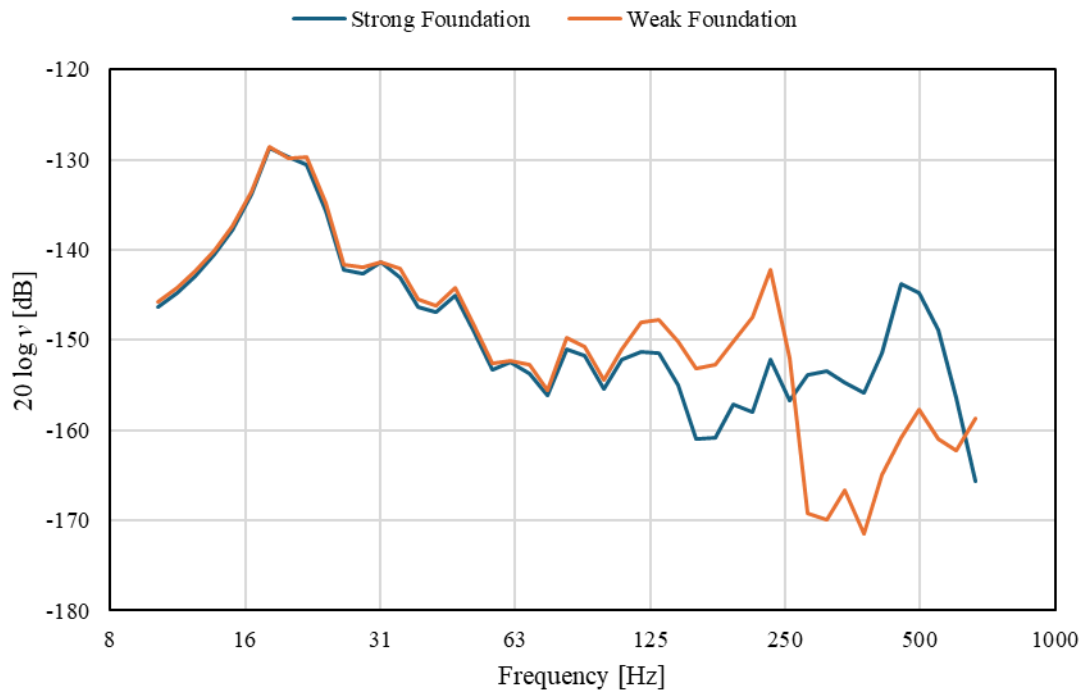


Figure 42. Frequency response foundation at the engine foundation.

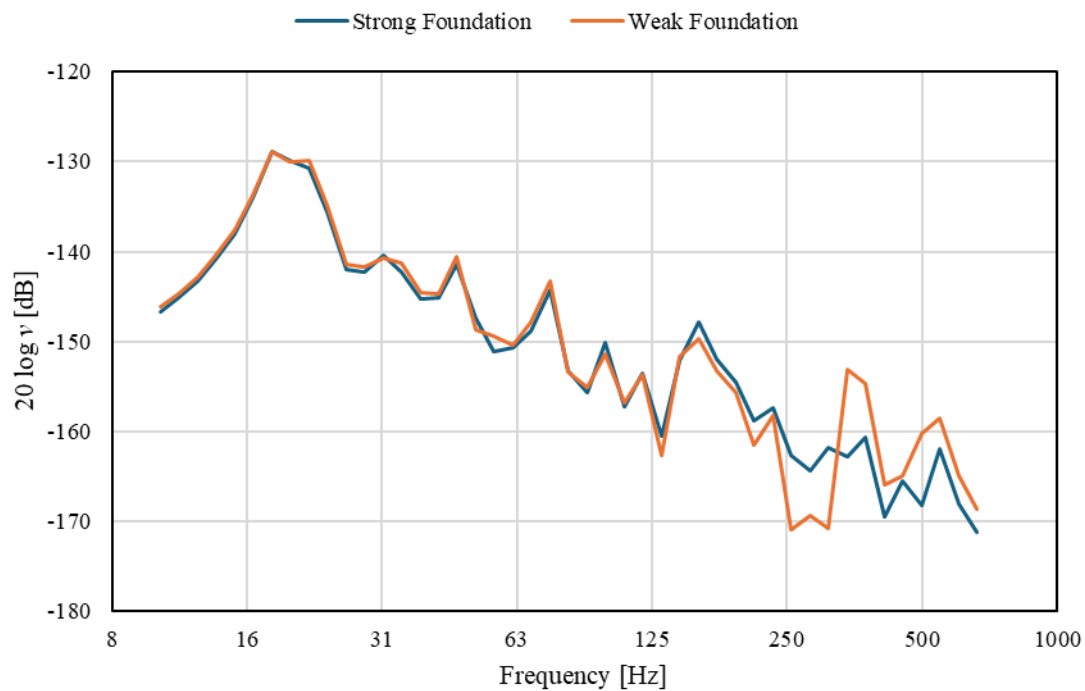


Figure 43. Frequency response foundation at the effective source area.

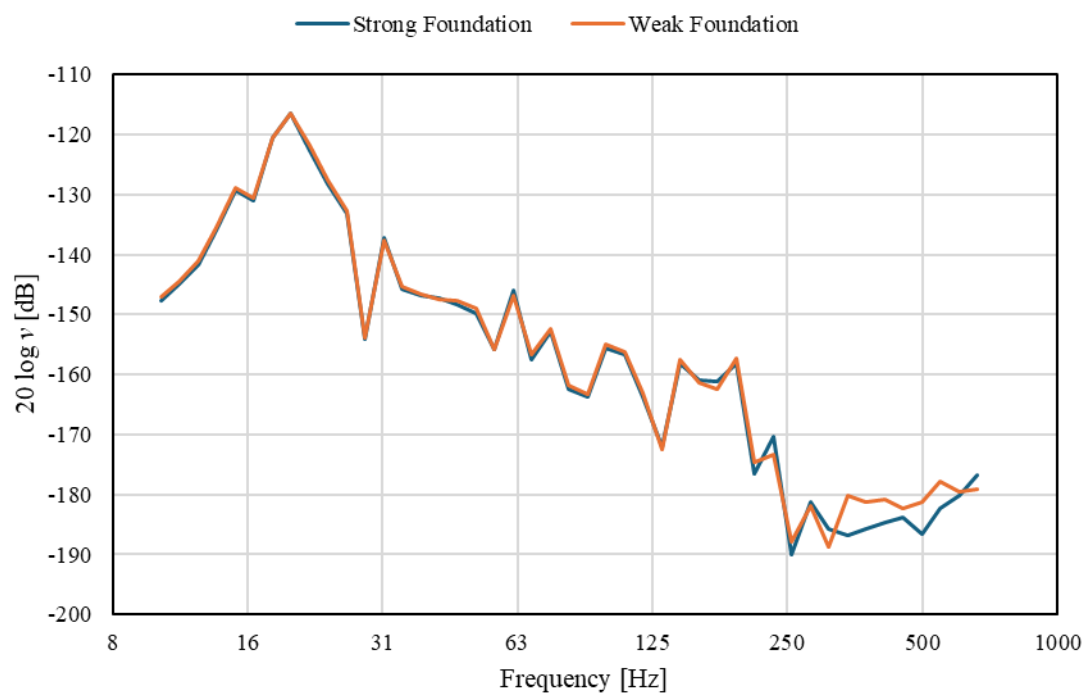


Figure 44. Frequency response foundation at deck (top).

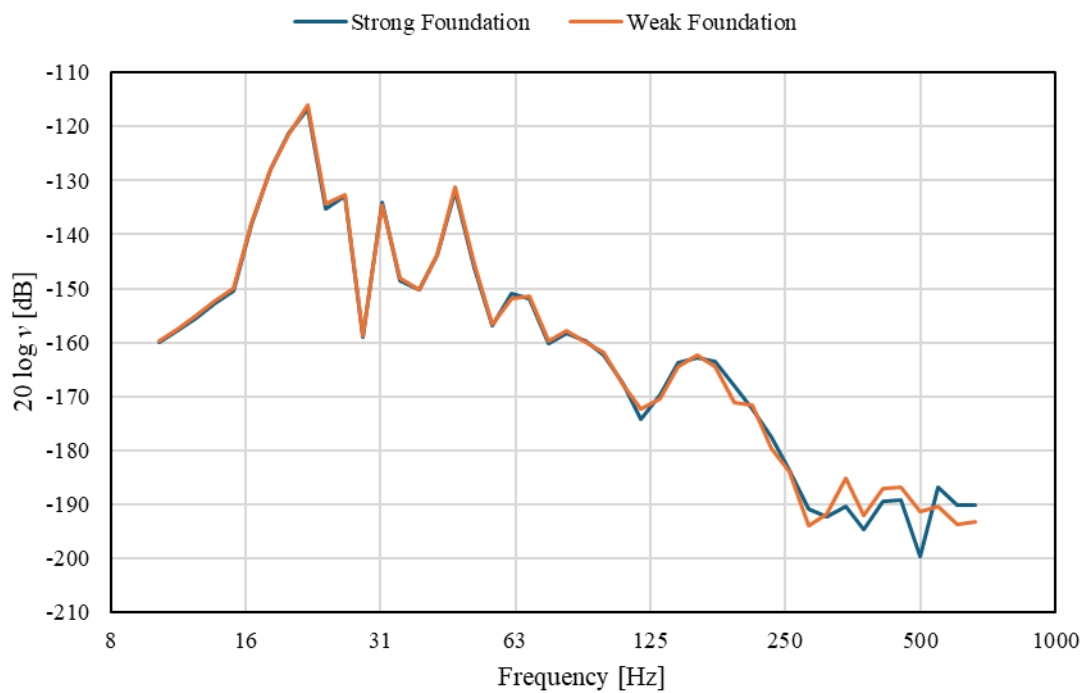


Figure 45. Frequency response foundation at deck (side).

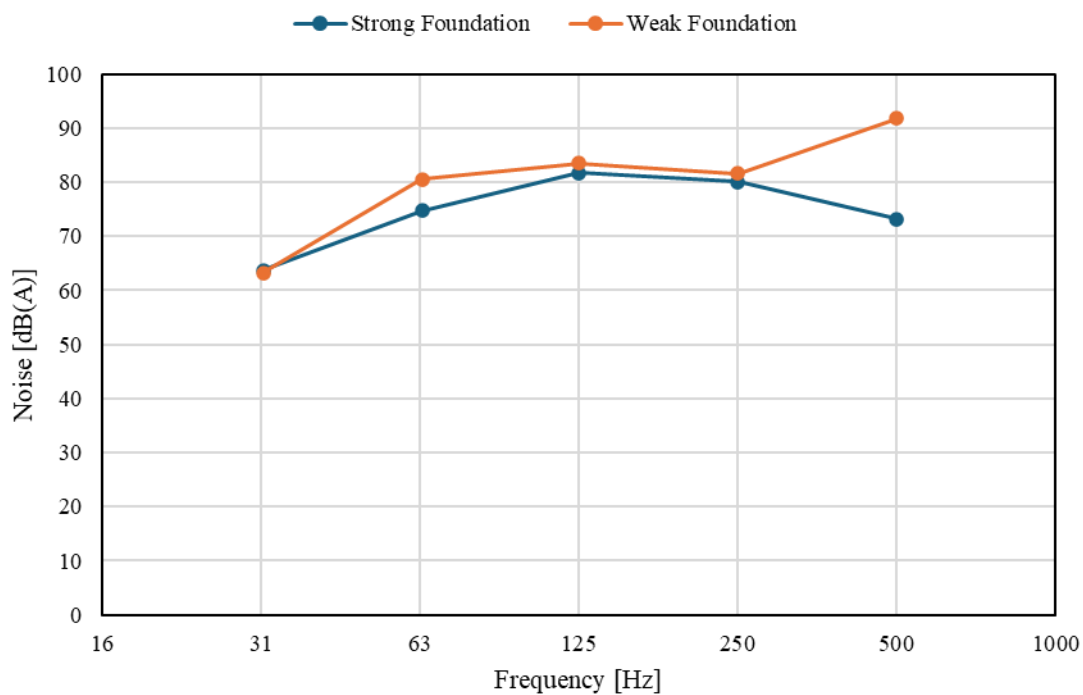


Figure 46. Airborne noise on deck (top) for both foundations.

The results (Fig. 42-43-44-45-46) show two big conclusions. There is a change of the foundation response (Fig. 42), specifically at high frequencies. Therefore, the transmission of noise between the top of the engine foundation and the effective source area is modified. For the other locations the transmission of noise is not modified since the curves for both cases are almost superimposed (Fig. 43-44-45). Comparing the airborne noise on deck (top) for both foundations (Fig. 46), the result is as expected which is an increment of noise for the weak foundation as the scantlings are reduced. For the octave band of 500 Hz (Fig. 46), there is a big increment of noise. For the weak foundation case (Fig. 47), at high frequencies, the response in the foundation is closer to the response in the effective source area and hence the noise attenuation is lower compared to the strong foundation case (Fig. 18).

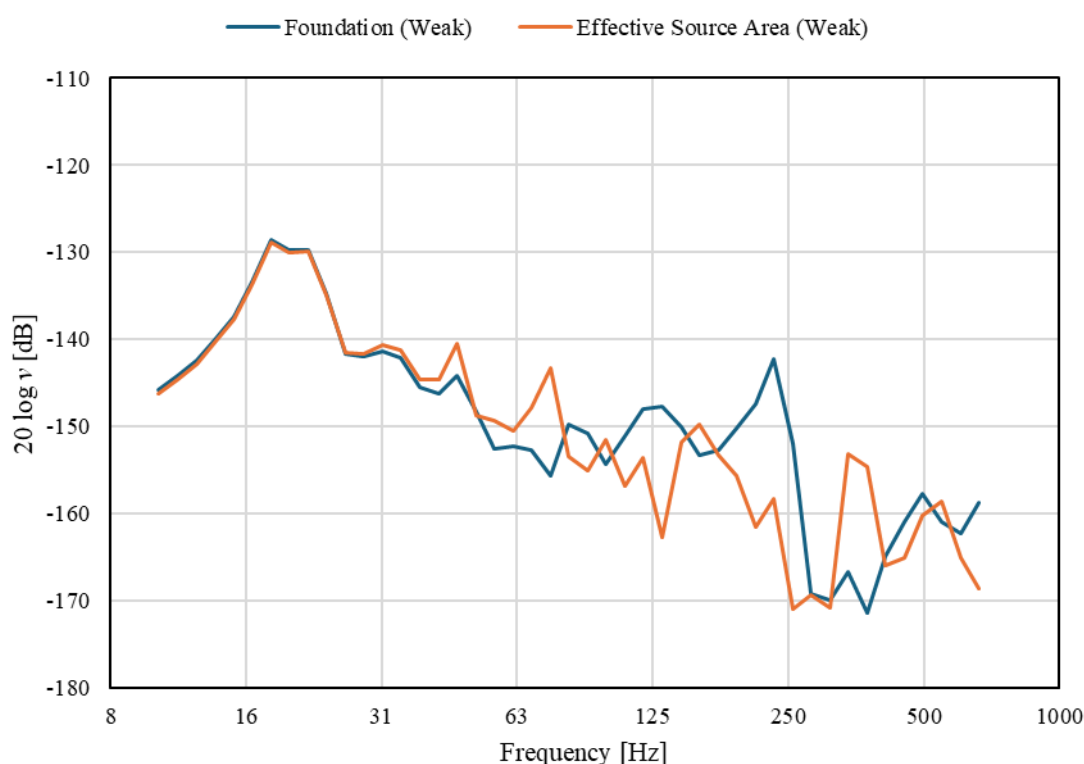


Figure 47. Frequency response function: weak foundation and effective source area.

In order to verify that the changes in the foundation do not violate the required noise limits the A-weighted sound pressure levels from Figure 46 are compared with the values from Table 7. As the space under study is a machinery space the noise level limit is 110 dB(A). Clearly, the results from both foundations are below the required limit and satisfy the criteria.

4. CONCLUSIONS

The results from the finite element method allow to highlight the limitations of the empirical method developed by SNAME for the octave bands below 125 Hz. The results estimated by SNAME for the octave bands below 125 Hz are very optimistic compared with the results provided by the finite element method. The extrapolation of information and scaling laws from high frequency data is not an accurate way to estimate the noise for lower frequencies.

It is important to highlight that the SNAME's procedure can provide results in question of minutes which proves that the analytical procedure is a good tool for the early design stage if it is applied in the proper range of frequencies. The finite element method allows to perform a very detailed analysis of the structure identifying the resonant frequencies of the structure which should be avoided. However, due to the computational cost of this method and the time required to its preparation the finite element method is more suitable for advanced design stages.

A complete methodology to study the limit conditions in shipboard machinery installation has been developed. Based on the response of both foundations, the structure-borne noise amplification is determined. This study allows to identify if changes in the machinery foundation violate the required noise limits.

The comparison of the response of the structure for both foundations allow to study how changes in the engine foundation influence the structure-borne propagation in the entire structure. The results show that the noise propagation is influenced in the vicinity of the foundation which is the expected result.

As future work, it would be of interest to apply the exact meshing criteria defined to represent properly the bending wavelengths for higher frequencies. The octave bands of 250 Hz and 500 Hz should be analysed with a finer mesh, especially in the case of the weak foundation to explain what is happening in the foundation for the octave band of 500 Hz.

5. REFERENCES

- ABS. (2019). *GUIDANCE NOTES ON ONBOARD NOISE ANALYSIS*. Spring, TX 77389 USA: ABS.
- ANSYS1. (2017). Retrieved from https://www.mm.bme.hu/~gyebro/files/ans_help_v182/ans_thry/thy_anproc4.html
- ANSYS2. (2017). Retrieved from https://www.mm.bme.hu/~gyebro/files/ans_help_v182/ans_elem/Hlp_E_ShellElements.html
- ANSYS3. (2017). Retrieved from https://www.mm.bme.hu/~gyebro/files/ans_help_v182/ans_elem/Hlp_E_BEAM188.html
- ANSYS4. (2017). Retrieved from https://www.mm.bme.hu/~gyebro/files/ans_help_v182/ans_elem/Hlp_E_ElemTOC.html
- MECHEAD. (2023). Retrieved from <https://www.mechead.com/mesh-quality-checking-ansys-workbench/>
- SIEMENS. (2019). Retrieved from https://support.sw.siemens.com/en-US/okba/KB000036272_EN_US/Natural-Frequency-and-Resonance/index.html
- SNAME. (2019). *Design Guide for Shipboard Airborne Noise Control*. Alexandria: SNAME.
- Wittekind, D. D. (2024). *Internal References*. Schwentimental, Germany: DW-ShipConsult GmbH.